



International Agreement Report

Assessment of the Wall Film Condensation Model with Non-condensable Gas in RELAP5 and TRACE for Vertical Tube and Plate Geometries

Prepared by:

Jehee Lee*, Chi-Jin Choi*, Hyoung Kyu Cho*, Kyung Won Lee**, Min Ki Cho**

*Department of Nuclear Engineering,
Seoul National University
1 Gwanak-ro, Gwanak-gu, Seoul, 08826, Republic of Korea

**Korea Institute of Nuclear Safety
62 Gwahak-ro, Yuseong-gu, Daejeon 34142, Republic of Korea

K. Tien, NRC Project Manager

**Division of Systems Analysis
Office of Nuclear Regulatory Research
U.S. Nuclear Regulatory Commission
Washington, DC 20555-0001**

Manuscript Completed: August 2017
Date Published: February 2019

Prepared as part of
The Agreement on Research Participation and Technical Exchange
Under the Thermal-Hydraulic Code Applications and Maintenance Program (CAMP)

**Published by
U.S. Nuclear Regulatory Commission**

AVAILABILITY OF REFERENCE MATERIALS IN NRC PUBLICATIONS

NRC Reference Material

As of November 1999, you may electronically access NUREG-series publications and other NRC records at NRC's Library at www.nrc.gov/reading-rm.html. Publicly released records include, to name a few, NUREG-series publications; *Federal Register* notices; applicant, licensee, and vendor documents and correspondence; NRC correspondence and internal memoranda; bulletins and information notices; inspection and investigative reports; licensee event reports; and Commission papers and their attachments.

NRC publications in the NUREG series, NRC regulations, and Title 10, "Energy," in the *Code of Federal Regulations* may also be purchased from one of these two sources.

1. The Superintendent of Documents

U.S. Government Publishing Office
Mail Stop IDCC
Washington, DC 20402-0001
Internet: bookstore.gpo.gov
Telephone: (202) 512-1800
Fax: (202) 512-2104

2. The National Technical Information Service

5301 Shawnee Road
Alexandria, VA 22312-0002
www.ntis.gov
1-800-553-6847 or, locally, (703) 605-6000

A single copy of each NRC draft report for comment is available free, to the extent of supply, upon written request as follows:

Address: **U.S. Nuclear Regulatory Commission**
Office of Administration
Multimedia, Graphics, and Storage &
Distribution Branch
Washington, DC 20555-0001
E-mail: distribution.resource@nrc.gov
Facsimile: (301) 415-2289

Some publications in the NUREG series that are posted at NRC's Web site address www.nrc.gov/reading-rm/doc-collections/nuregs are updated periodically and may differ from the last printed version. Although references to material found on a Web site bear the date the material was accessed, the material available on the date cited may subsequently be removed from the site.

Non-NRC Reference Material

Documents available from public and special technical libraries include all open literature items, such as books, journal articles, transactions, *Federal Register* notices, Federal and State legislation, and congressional reports. Such documents as theses, dissertations, foreign reports and translations, and non-NRC conference proceedings may be purchased from their sponsoring organization.

Copies of industry codes and standards used in a substantive manner in the NRC regulatory process are maintained at—

The NRC Technical Library

Two White Flint North
11545 Rockville Pike
Rockville, MD 20852-2738

These standards are available in the library for reference use by the public. Codes and standards are usually copyrighted and may be purchased from the originating organization or, if they are American National Standards, from—

American National Standards Institute

11 West 42nd Street
New York, NY 10036-8002
www.ansi.org
(212) 642-4900

Legally binding regulatory requirements are stated only in laws; NRC regulations; licenses, including technical specifications; or orders, not in NUREG-series publications. The views expressed in contractor prepared publications in this series are not necessarily those of the NRC.

The NUREG series comprises (1) technical and administrative reports and books prepared by the staff (NUREG-XXXX) or agency contractors (NUREG/CR-XXXX), (2) proceedings of conferences (NUREG/CP-XXXX), (3) reports resulting from international agreements (NUREG/IA-XXXX), (4) brochures (NUREG/BR-XXXX), and (5) compilations of legal decisions and orders of the Commission and Atomic and Safety Licensing Boards and of Directors' decisions under Section 2.206 of NRC's regulations (NUREG-0750).

DISCLAIMER: This report was prepared under an international cooperative agreement for the exchange of technical information. Neither the U.S. Government nor any agency thereof, nor any employee, makes any warranty, expressed or implied, or assumes any legal liability or responsibility for any third party's use, or the results of such use, of any information, apparatus, product or process disclosed in this publication, or represents that its use by such third party would not infringe privately owned rights.



International Agreement Report

Assessment of the Wall Film Condensation Model with Non-condensable Gas in RELAP5 and TRACE for Vertical Tube and Plate Geometries

Prepared by:

Jehee Lee*, Chi-Jin Choi*, Hyoung Kyu Cho*, Kyung Won Lee**, Min Ki Cho**

*Department of Nuclear Engineering,
Seoul National University
1 Gwanak-ro, Gwanak-gu, Seoul, 08826, Republic of Korea

**Korea Institute of Nuclear Safety
62 Gwahak-ro, Yuseong-gu, Daejeon 34142, Republic of Korea

K. Tien, NRC Project Manager

**Division of Systems Analysis
Office of Nuclear Regulatory Research
U.S. Nuclear Regulatory Commission
Washington, DC 20555-0001**

Manuscript Completed: August 2017

Date Published: February 2019

Prepared as part of
The Agreement on Research Participation and Technical Exchange
Under the Thermal-Hydraulic Code Applications and Maintenance Program (CAMP)

**Published by
U.S. Nuclear Regulatory Commission**

ABSTRACT

In the interest of providing increased power supply, available passive safety features such as Passive Containment Cooling System (PCCS) and Passive Auxiliary Feedwater System (PAFS) have been adopted for use in advanced nuclear power reactors. The accurate prediction of condensation heat transfer in these systems has been emphasized to assure the safety of nuclear reactors. Especially in the PCCS, condensation occurs in the presence of non-condensable gases that concentrate on the condenser wall. The concentrated gases reduce the steam partial pressure and degrade the heat transfer rate.

In order to predict the condensation rate under this condition, RELAP5 (which is generally used for simulation of best-estimate transients in light water reactor coolant systems) uses the Colburn-Hougen model. Recently, it was found that an error was included in the condensation mass flux model of RELAP5, and the source code of the model was corrected. Next, it was necessary to assess the predictive capability of the corrected model in relation to existing experimental results and in relation to results predicted using another code.

In this study, seven condensation experiments were simulated using RELAP5 and TRACE. These were used to describe condensation on the inner wall of the channel in the presence of non-condensable gases. Then, the predicted heat flux and heat transfer coefficient from both codes were compared with experimental results to evaluate the condensation models.

TABLE OF CONTENTS

ABSTRACT	iii
LIST OF FIGURES	vii
LIST OF TABLES	ix
EXECUTIVE SUMMARY	xi
ACKNOWLEDGMENTS	xiii
ABBREVIATIONS AND ACRONYMS	xv
1 INTRODUCTION	1-1
2 ERROR CORRECTION OF WALL FILM CONDENSATION MODEL IN RELAP5.....	2-1
3 RELAP5 ASSESSMENT RESULTS	3-1
3.1 Analysis of the COPAIN Experiment	3-1
3.2 Analysis of the University of Wisconsin Experiment	3-5
3.3 Analysis of the CONAN Experiment	3-9
3.4 Analysis of the MIT Experiments	3-13
3.5 Analysis of the KAIST Experiment	3-17
3.6 Analysis of the POSTECH Experiment.....	3-21
3.7 Analysis of the UCB Experiments	3-25
3.8 Synthesis of the Analysis Results	3-29
4 TRACE ASSESSMENT RESULTS	4-1
4.1 Analysis of the COPAIN Experiment	4-4
4.2 Analysis of the UW Experiment.....	4-5
4.3 Analysis of the CONAN Experiment	4-7
4.4 Analysis of the MIT Experiment.....	4-10
4.5 Analysis of the KAIST Experiment	4-11
4.6 Analysis of the POSTECH Experiment.....	4-11
4.7 Analysis of the UCB Experiment	4-13

5	CONCLUSIONS.....	5-1
6	REFERENCES.....	6-1

LIST OF FIGURES

Figure 1	Film Condensation Schematic (Ref. 2).....	1-2
Figure 2	Schematic Diagram of COPAIN Experiment (Ref. 9).....	3-2
Figure 3	COPAIN Simulation Nodalization and Node Convergence Result.....	3-3
Figure 4	COPAIN Calculation Results (RELAP5).....	3-4
Figure 5	Comparison of COPAIN Experimental and Calculated Results	3-5
Figure 6	Schematic Diagram of UW Experiment (Ref. 10)	3-6
Figure 7	UW Simulation Nodalization and Node Convergence Result	3-7
Figure 8	UW Calculation Results (RELAP5)	3-8
Figure 9	Comparison of the UW Experimental and Calculated Results	3-9
Figure 10	Schematic Diagram of the CONAN Experiment (Ref. 11).....	3-10
Figure 11	Results of the CONAN Simulation Nodalization and Node Convergence	3-11
Figure 12	CONAN Calculation Results (RELAP5).....	3-12
Figure 13	Results of the CONAN Experimental and Calculated Results	3-13
Figure 14	Schematic Diagram of the MIT Experiment (Ref. 12)	3-13
Figure 15	MIT Simulation Nodalization	3-15
Figure 16	MIT Calculation Results (RELAP5)	3-16
Figure 17	Comparison of the MIT Experimental and Calculated Results (RELAP5).....	3-17
Figure 18	Schematic Diagram of the KAIST Experiment (Ref. 13)	3-18
Figure 19	KAIST Simulation Nodalization	3-19
Figure 20	KAIST Calculation Results (RELAP5)	3-20
Figure 21	Comparison of the KAIST Experimental and Calculated Results.....	3-21
Figure 22	Schematic Diagram of the POSTECH Experiment (Ref. 14)	3-21
Figure 23	POSTECH Simulation Nodalization.....	3-23
Figure 24	POSTECH Calculation Results (RELAP5)	3-24
Figure 25	Comparison of POSTECH Experimental and Calculated Results.....	3-25
Figure 26	Schematic Diagram of the UCB Experiment (Ref. 10).....	3-25
Figure 27	UCB Simulation Nodalization	3-27
Figure 28	UCB Calculation Results.....	3-28
Figure 29	Comparison of UCB Experimental and Calculated Results	3-29
Figure 30	Heat Flux Comparison Results (Forced Convection).....	3-30
Figure 31	Heat Transfer Coefficient Comparison Results (Forced Convection).....	3-31
Figure 31	Heat Flux Comparison Results (Natural Convection)	3-31
Figure 33	Heat Transfer Coefficient Results (Natural Convection)	3-32
Figure 34	Plate Condensation Error: Experimental vs Simulation	3-32
Figure 35	COPAIN P0443 Test TRACE Analysis Result (With Hydraulic Diameter)	4-2
Figure 36	Schematic of Heated Length Calculation Method in Tube and Plate Wall	4-3
Figure 37	COPAIN P0443 Test TRACE Analysis Result (With Heated Diameter).....	4-4
Figure 38	COPAIN Calculation Results (TRACE)	4-5
Figure 39	UW Calculation Results (TRACE)	4-6
Figure 40	CONAN Calculation Results (TRACE)	4-8
Figure 41	Comparison of RELAP5 and TRACE Results (Plate Experiment)	4-9
Figure 42	MIT Calculation Results (TRACE).....	4-10
Figure 43	KAIST Calculation Results (TRACE).....	4-11
Figure 44	POSTECH Calculation Results (TRACE).....	4-12
Figure 45	UW Calculation Results (TRACE)	4-13
Figure 46	Comparison of RELAP5 and TRACE Results (Tube Experiment)	4-14

LIST OF TABLES

Table 1	Experimental Conditions Used for the RELAP5 Validation	3-1
Table 2	COPAIN Experimental Conditions.....	3-2
Table 3	Flow Regime of the COPAIN Calculation	3-4
Table 4	UW Experimental Conditions	3-6
Table 5	Flow Regime of the UW Calculation.....	3-9
Table 6	CONAN Experimental Conditions	3-10
Table 7	MIT Experimental Conditions	3-14
Table 8	Flow Regime of the MIT Calculation	3-17
Table 9	KAIST Experimental Conditions	3-18
Table 10	Flow Regime of the KAIST Calculation	3-20
Table 11	POSTECH Experimental Conditions	3-22
Table 12	UCB Experimental Conditions.....	3-26
Table 13	Film Condensation Model Comparison Between RELAP5 and TRACE	4-1

EXECUTIVE SUMMARY

Passive safety features have been applied to advanced pressurized water reactors (PWRs) for safety enhancement due to the recognized importance of applying available passive safety features. In these safety systems, such as Passive Containment Cooling System (PCCS) and Passive Auxiliary Feedwater System (PAFS), condensation occurs inside or outside the wall of the heat exchanger. An accurate prediction of the condensation heat transfer rate through these heat exchangers is of great significance in evaluating the performance of the passive safety systems and the safety of the advanced PWRs in which these safety systems are installed.

RELAP5 includes the Colburn-Hougen model for the prediction of condensation heat transfer with non-condensable gases. However, it was found that an error was included in condensation mass flux model of RELAP5, which determines the condensation rate. For this reason, the error in the source code of the model was corrected. Next, it is necessary to assess the prediction capability of the corrected model using existing experimental results and using results predicted by another code. Therefore, in this study elementary validation calculations were performed in a bid to show enhancement of the prediction capability.

This report includes assessment results of wall condensation heat transfer by comparing seven condensation heat transfer experiments and RELAP5 simulation results using the modified wall condensation model. Most of the experimental data (except the entrance region) can be predicted using RELAP5 with an error within 30%. When analyzing the PCCS where condensation occurs with high NC gas quality, the corrected model can elevate the heat transfer rate prediction considerably. This makes it is desirable to apply the corrected model.

ACKNOWLEDGMENTS

This work was supported by the Korea Radiation Safety Foundation (KORSAFE) grant funded by the Korean government (NSSC) (Nuclear Safety Research Center Program: 1305011).

ABBREVIATIONS AND ACRONYMS

MELCOR	Methods for Estimation of Leakages and Consequences of Releases
PAFS	Passive Auxiliary Feedwater System
PCCS	Passive Containment Cooling System
PWR	Pressurized Water Reactor
RELAP	Reactor Excursion and Leak Analysis Program
TRACE	TRAC/RELAP Advanced Computational Engine

1 INTRODUCTION

The system analysis code RELAP5, which is used for the safety assessment of nuclear power plants, uses the Colburn-Hougen model (Ref. 1) for predicting wall-film condensation heat transfer in the presence of non-condensable gases (Ref. 2). As shown in Figure 1, the model uses the vapor fraction, liquid film, and non-condensable gas boundary layer in the presence of a non-condensable gas mixture, to calculate the condensation mass flux and the wall heat flux. In RELAP5, the sensible heat transfer between interface and gas is not considered, contrary to the original Colburn-Hougen model; thus, the model predicts the condensation heat transfer from the energy conservation equation at the liquid–gas interface as shown in the equation below:

$$h_c (T_{vi} - T_w) = h_{fg} j_v ,$$

where h_c = liquid film heat transfer coefficient (W/m²·K),

h_{fg} = latent heat (J/kg),

j_v = vapor mass flux (kg/m²·s),

T_{vi} = interface temperature (K),

T_w = wall temperature (K).

The Colburn-Hougen model should be solved using an iterative method because it treats the temperature and vapor partial pressure at the interface as unknowns. When the iterations are converged, the temperature at the interface, partial pressure of steam, and non-condensable gas fraction can be obtained from the model. Many nuclear safety analysis codes, such as RELAP5 (Ref. 2), TRACE (Ref. 3), and MELCOR (Ref. 4) have adopted the Colburn-Hougen model as their wall condensation heat transfer model in the presence of non-condensing gases with some modifications. This is because variables at the interface can be obtained mechanistically by using it.

In this report, the models used by the nuclear safety analysis codes RELAP5 and TRACE to predict wall-film condensation in the presence of non-condensable gases, are summarized and the differences between them analyzed. During this process, an error in the wall-film condensation model of RELAP5 was detected and its source code corrected. The modified code was validated against the data from seven experiments on wall-film condensation, wherein the test section geometries were vertical plates or tubes. Afterwards, validation was repeated using TRACE, and the differences in the calculation results were quantitatively analyzed.

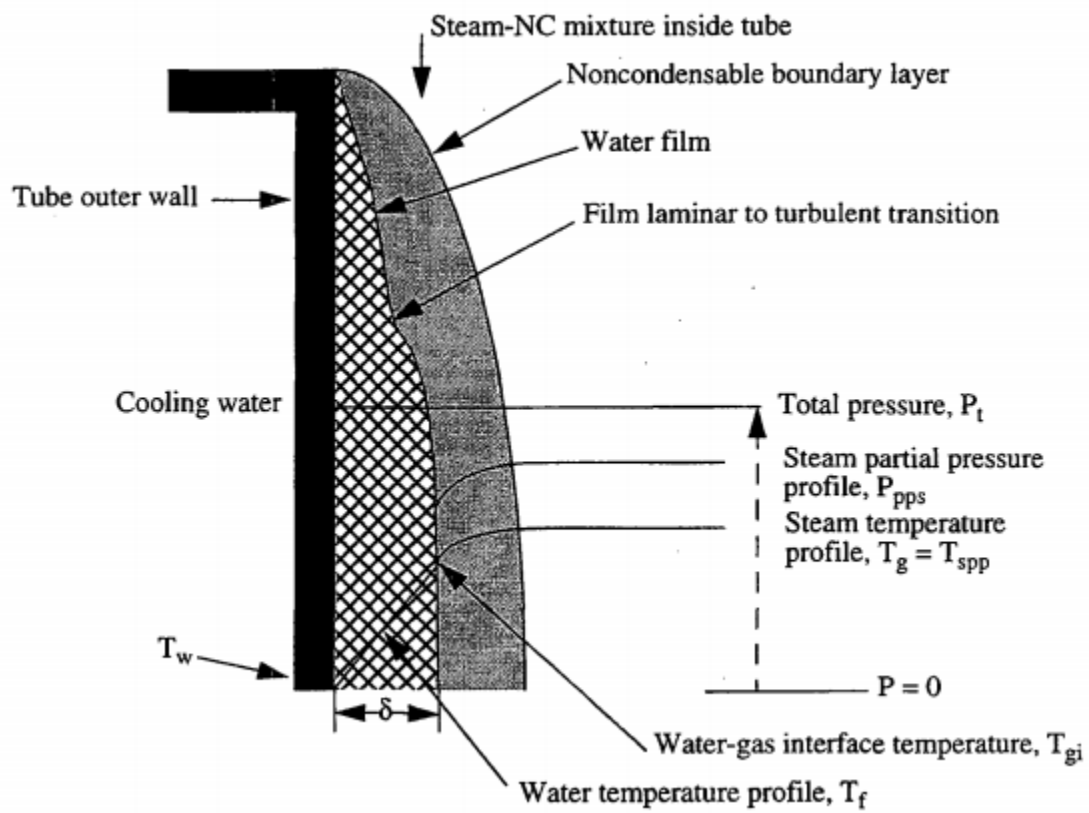


Figure 1 **Film Condensation Schematic (Ref. 2)**

2 ERROR CORRECTION OF WALL FILM CONDENSATION MODEL IN RELAP5

For the calculation of film condensation at the interface in the presence of non-condensable gases, RELAP5 and other codes use the Colburn-Hougen model. The Colburn-Hougen model calculates the heat transfer from the energy balance through the liquid/gas interface, and the sensible heat transfer between the gas and interface is not considered.

$$h_c (T_{vi} - T_w) = h_{fg} j_v = h_m \rho_{vb} \ln \left(\frac{1 - \frac{P_{vi}}{P}}{1 - \frac{P_{vb}}{P}} \right)$$

where j_v = vapor mass flux (kg/m²·s),

h_m = mass transfer coefficient (m/s),

ρ_{vb} = saturation vapor density at P_{vb} (kg/m³),

P = total pressure (Pa),

P_{vi} = partial pressure of steam at liquid/gas/vapor interface (Pa),

P_{vb} = partial pressure of steam at bulk stream (Pa).

To calculate the mass transfer coefficient, RELAP5 uses the Gilliland correlation (Ref. 5) for the forced-convection turbulent flow, and the Churchill-Chu correlation (Ref. 6) for the natural-convection flow.

The condensation mass flux term of RELAP5 is presented below,

$$j_v = h_m \rho_{vb} \ln \left(\frac{1 - \frac{P_{vi}}{P}}{1 - \frac{P_{vb}}{P}} \right)$$

In this equation, the condensation mass flux of RELAP5 is determined by the difference between P_{vi} and P_{vb} multiplied by vapor density and the mass transfer coefficient. RELAP5 uses the saturation vapor density at P_{vb} as a density term of the condensation mass flux. This definition is different from those in other codes and documents, and turned out to be physically incorrect. In general, the density term of the condensation mass flux is defined as the saturation vapor density at the total pressure and is expressed as ρ_{vb}/x_{vb} ; where x_{vb} means mole fraction in the bulk stream. This error might have been caused by a misinterpretation of the definition of density in the condensation mass flux during implementation of the condensation model in Ref. 7. For this reason, the original condensation model of RELAP5 under-predicts the

condensation heat transfer when wall condensation occurs in the presence of non-condensable gases, especially under high non-condensable gas quality condition. Therefore, the performance of the safety system incorporating the condensation heat transfer with non-condensable gases might not be properly evaluated. For this reason, the condensation heat flux term of RELAP5 was corrected from

$$q'' = h_m (h_{g,sat} - h_{f,sat}) \rho_{vb} \ln \left(\frac{P - P_{vi}}{P - P_{vb}} \right),$$

to

$$q'' = h_m (h_{g,sat} - h_{f,sat}) \left(\frac{\rho_{vb}}{x_{vb}} \right) \ln \left(\frac{P - P_{vi}}{P - P_{vb}} \right).$$

This correction was implemented in the latest version of RELAP5 (ver. 3.x ki, released in 2015) (Ref. 8).

3 RELAP5 ASSESSMENT RESULTS

After modifying the wall-film condensation model of RELAP5, the COPAIN (Ref. 9), UW (Ref. 10), CONAN (Ref. 11), MIT (Ref. 12), KAIST (Ref. 13), POSTECH (Ref. 14), and UCB (Ref. 10) experiments were simulated to investigate the effect of the modification and the difference in the condensation heat flux results that depend on the wall-film condensation model. The geometries of the test sections and the experimental conditions of the tests are summarized in Table 1. Among the results presented in each experiment, the test conditions that give the wall temperatures as boundary conditions were used in this assessment. This is because the prediction errors of the cooling-jacket heat removal performance and those of the condensation heat transfer rate coexist, which makes the error analysis originating from the condensation model complicated.

Table 1 Experimental Conditions Used for the RELAP5 Validation

	COPAIN	Univ. of Wisconsin	CONAN	Siddique (1993)	Park (1999)	Lee (2008)	Kuhn (1997)
	CEA	UW	UP	MIT	KAIST	POSTECH	UCB
Test section geometry/ Condensing surface	Rectan- gular duct/ Plate wall	Rectan- gular duct/ Plate wall	Rectan- gular duct/ Plate wall	Tube/ Inner wall	Tube/ Inner wall	Tube/ Inner wall	Tube/ Inner wall
Length (m)	2.0	1.07	2.0	2.54	2.4	2.8	2.4
Tube ID or Duct size (mm)	600 ×500	152.4 ×152.4	340 ×340	46	47.5	13	47.5
NC Gas type	Air helium	Air	Air	Air helium	Air	Nitrogen	Air helium
Steam flow	0.1 - 3.0 (m/s)	1.0 - 3.0 (m/s)	1.5 - 3.5 (m/s)	2.4 - 8.9 (g/s)	2 - 11 (g/s)	1.8 - 7.8 (g/s)	8.2 - 17 (g/s)
Inlet NC mass fraction (%)	0 - 100	0 - 80	0 - 75	10 - 35	10 - 70	0 - 40	0 - 40
Pressure (MPa)	0.1	0.1	0.1	0.1 - 0.5	0.17	0.1 - 0.13	0.1 - 0.4

3.1 Analysis of the COPAIN Experiment

Among the COPAIN condensation experiments (Ref. 9) conducted at CEA, the P0441, P0443, P0444, and P0344 experiments were analyzed to assess the modified RELAP5. The

experimental conditions and schematic diagram of the experimental apparatus are presented in Table 2 and Figure 2.

For the RELAP5 calculation, the nodalization of the COPAIN experiment was constructed as shown in Figure 3. The gas mixture was injected from the time dependent volume-100 located at the top of pipe-300. The gas mixture passed through the time dependent junction-150, and then entered pipe-300, where condensation occurred. Pipe-300 had 12 volumes for the gas mixture flow. No heat was exchanged at volume 300-1 and 300-12, and the heat exchange with the wall occurred in the other 10 volumes between them. The gas mixture then flowed out to the time dependent volume-500. The heat exchanger was simulated using the heat structure H-300, and constant wall temperature conditions were imposed on the condensing wall with respect to the experimental conditions summarized in Table 2.

Table 2 COPAIN Experimental Conditions

	P0441	P0443	P0444	P0344
Inlet gas velocity	3.0 m/s	1.0 m/s	0.5 m/s	0.3 m/s
Outlet pressure	1.02 bar	1.02 bar	1.02 bar	1.21 bar
Inlet gas temperature	353.2 K	352.3 K	351.5 K	344.0 K
Wall temperature	307.4 K	300.1 K	299.7 K	322.0 K
Air mass fraction	0.767	0.772	0.773	0.864

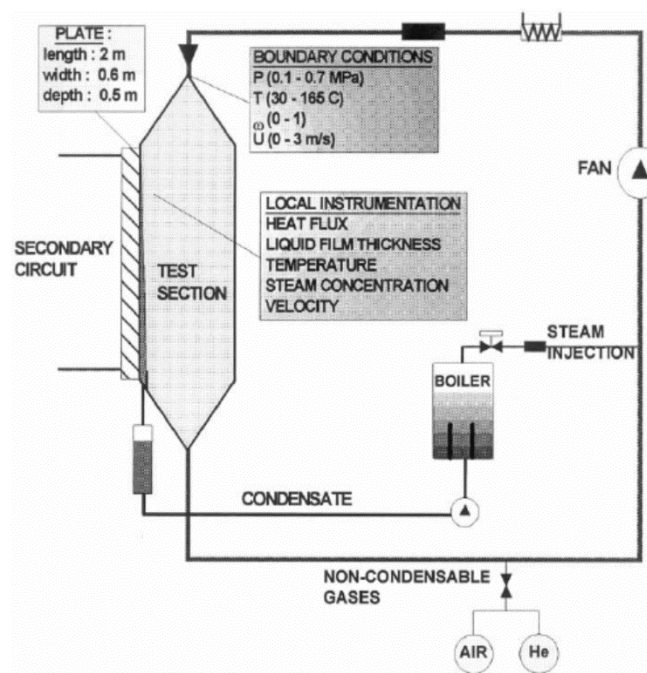


Figure 2 Schematic Diagram of COPAIN Experiment (Ref. 9)

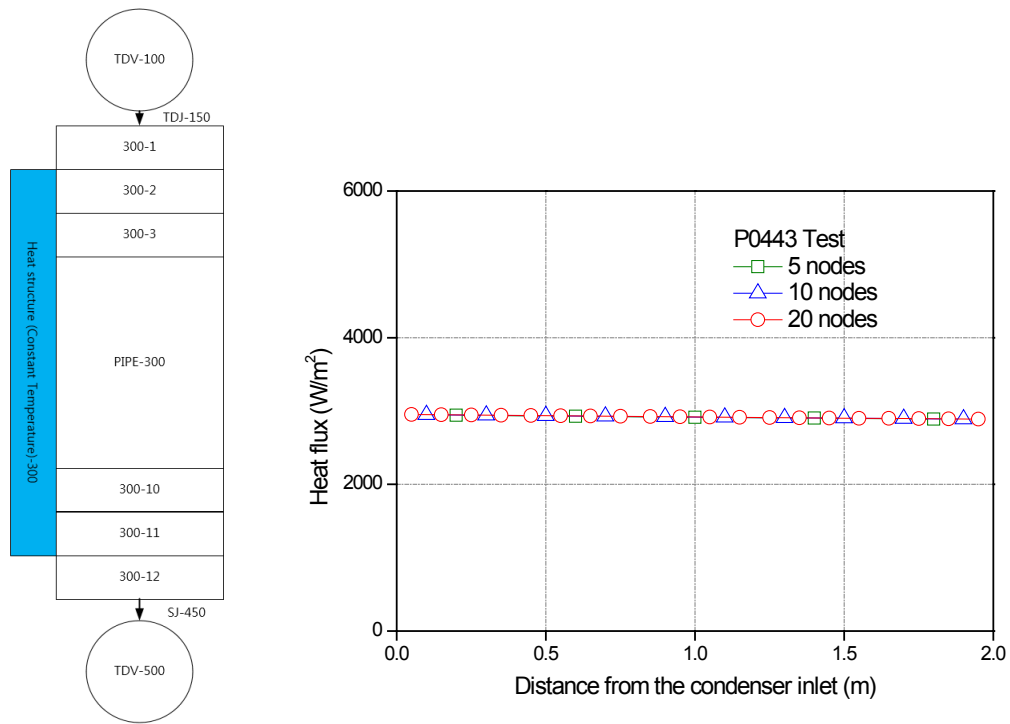


Figure 3 COPAIN Simulation Nodalization and Node Convergence Result

Figure 4 shows the results of the analysis using the original and modified RELAP5. As shown in Figure 4, the original RELAP5 underestimates the condensation mass flux and thus, underpredicts the heat flux. After modification of the wall-film condensation model, the heat flux results increased, and the discrepancy in the experiment results was reduced. Near the entrance region, the predicted heat flux was significantly lower than the experimental data because the heat transfer model was developed for a fully developed flow. This limitation of the one-dimensional analysis code, which uses heat transfer coefficients, could be addressed if a multiplication factor for the entrance region were adopted in the future.

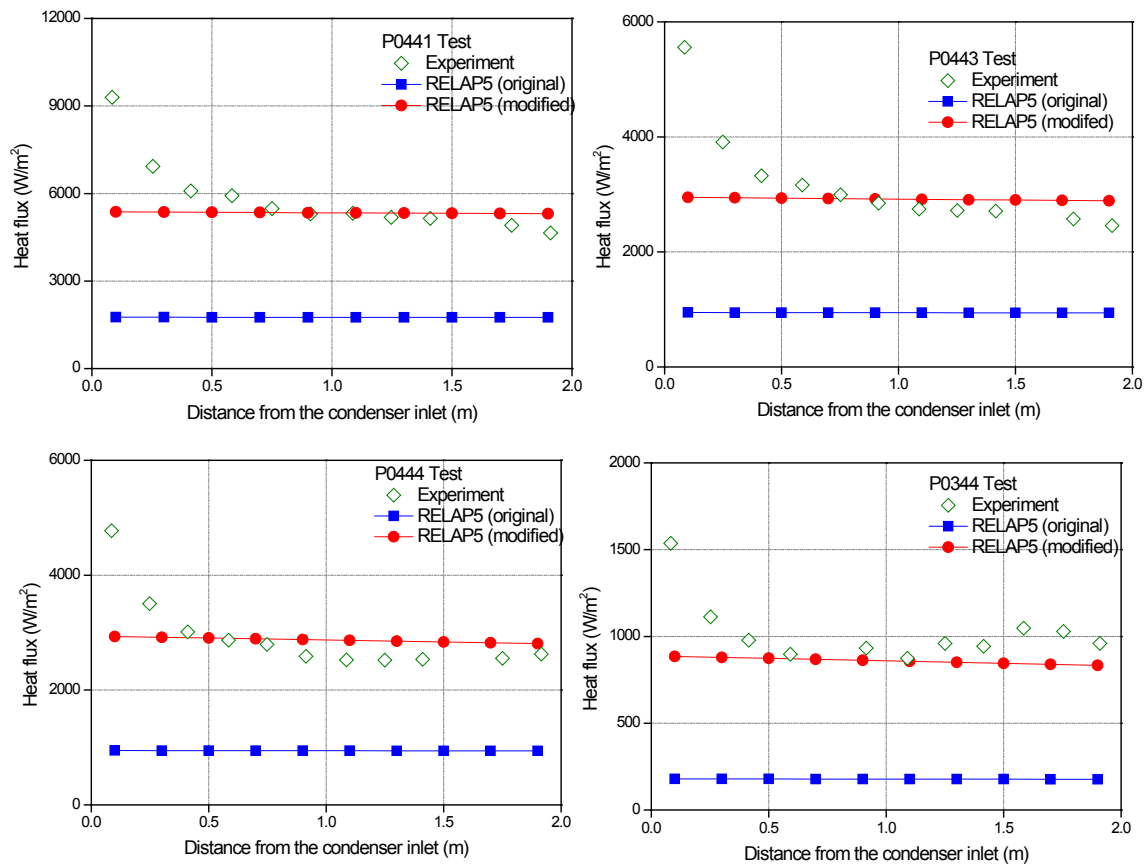


Figure 4 COPAIN Calculation Results (RELAP5)

Table 3 shows the flow regime in the calculation, and Figure 5 shows the calculation error according to the flow regime. In the COPAIN calculation, the heat flux results were significantly increased in the modified RELAP5 owing to the high non-condensable gas mass fraction. Therefore, the error of the modified RELAP5 was significantly lowered, and the error was predicted to be within 25%, excluding the entrance region ($L/D < 0.2$).

Table 3 Flow Regime of the COPAIN Calculation

Test #	Forced convection turbulent flow	Natural convection flow
P0441	O	
P0443		O
P0444		O
P0344		O

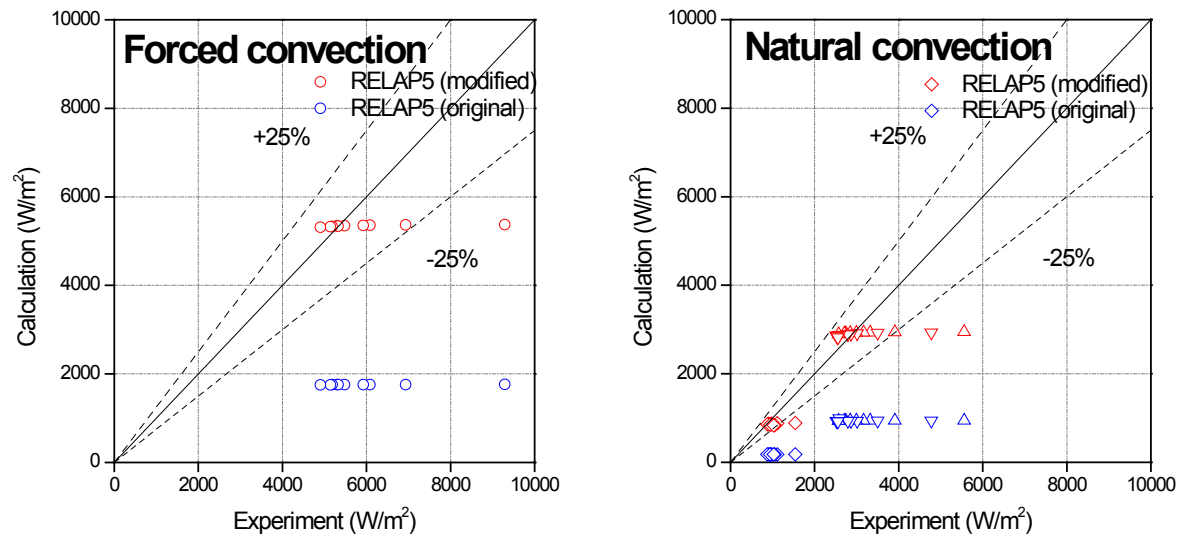


Figure 5 Comparison of COPAIN Experimental and Calculated Results

3.2 Analysis of the University of Wisconsin Experiment

For further assessment of the condensation model for rectangular channels, the condensation experiment performed at the University of Wisconsin was analyzed using RELAP5. For the RELAP5 calculation, the experimental conditions used were adopted from the TRACE Code Evaluation Manual (Ref. 10). The experimental conditions and schematic diagram of the experimental apparatus are presented in Table 4 and Figure 6.

For the RELAP5 calculation, the calculation node for the UW experiment was constructed as shown in Figure 7. In Figure 7, the gas mixture was injected from the time dependent volume-95, located at the top of pipe-110. The gas mixture passed through time dependent junction-100, and then entered pipe-110, where condensation occurred. Pipe-110 had 9 volumes for the gas mixture flow. No heat was exchanged between volume 110-1 and 110-9, and the heat exchange with the wall occurred in the remaining 7 volumes. The gas mixture then flowed out to the time dependent volume-125. The heat exchanger was simulated using the heat structure H-110, and constant wall temperature conditions were imposed on the condensing wall with respect to the experimental conditions summarized in Table 4

Table 4 UW Experimental Conditions

Test #	ΔT (K)	Air mass fraction	Inlet gas velocity (m/s)
1	40	0.778	1
2	40	0.778	3
3	50	0.640	1
4	50	0.640	3
5	60	0.405	1
6	50	0.225	1

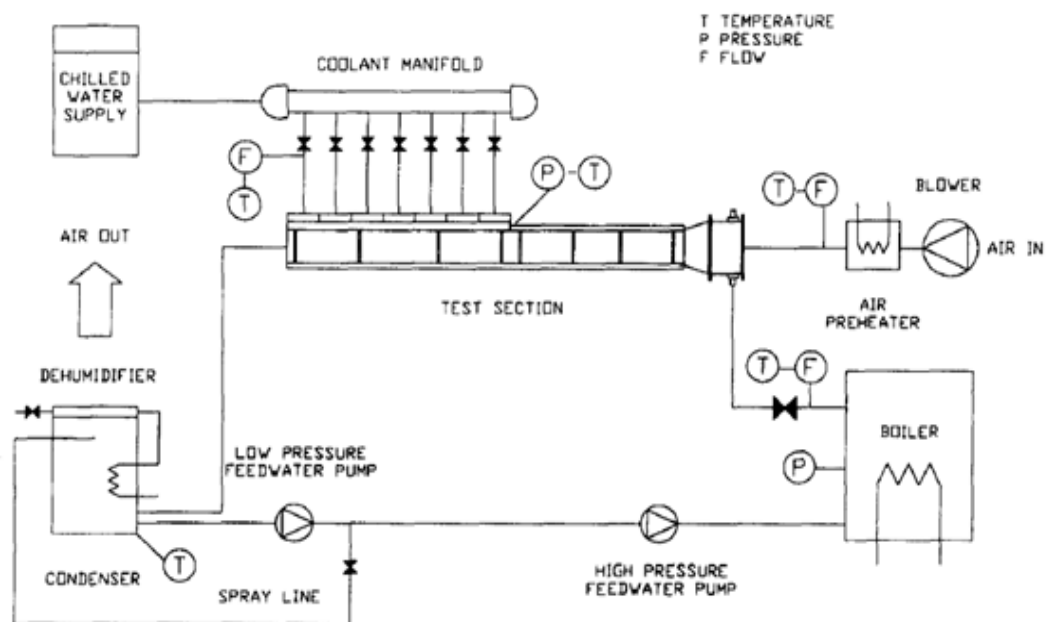


Figure 6 Schematic Diagram of UW Experiment (Ref. 10)

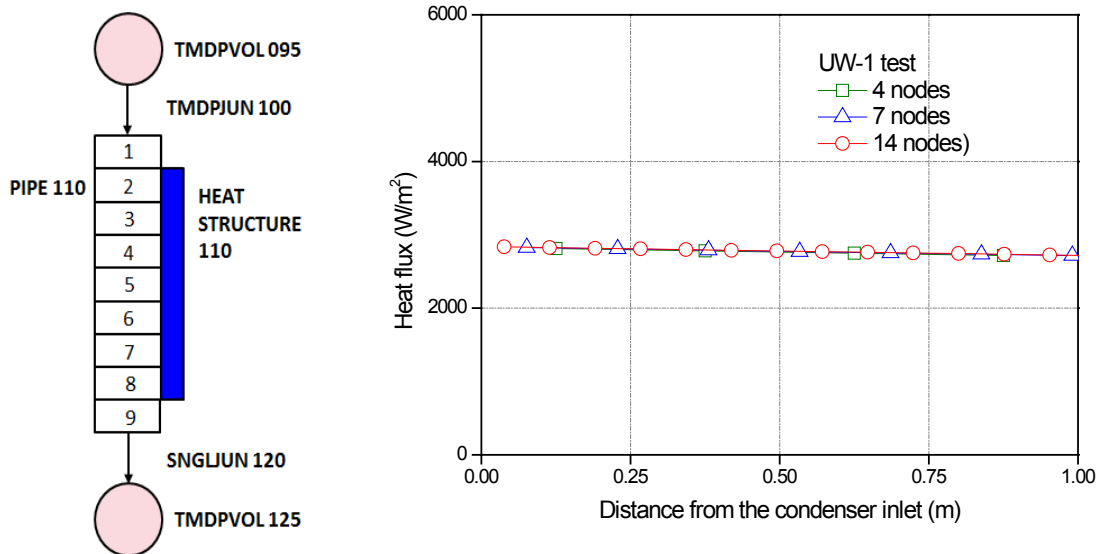


Figure 7 UW Simulation Nodalization and Node Convergence Result

Figure 8 shows the calculation results using the original and modified RELAP5. The heat-transfer coefficient results of RELAP5 were compared with the overall heat transfer coefficients of the experiment because they were only available in Ref. 10. As shown in Figure 8, the original RELAP5 under-predicts the condensation rate and under-estimates the heat transfer coefficient accordingly. After modification of the wall condensation model, the condensation heat-transfer coefficient of the RELAP5 increased and the prediction became closer to the experimental results, but was still lower. One of the reasons for this under-predicted heat transfer coefficient is that the overall heat transfer coefficients were used for the comparison and they can be influenced by the entrance effect. As shown in the previous COPAIN experiment calculation, a general calculation result of the plate condensation experiment is that the heat transfer coefficient is very high in the entrance region. Because the entrance effect can contribute to increase in the estimated overall heat transfer coefficient, it can cause under-prediction of the local heat transfer coefficients by RELAP5.

Table 5 presents the flow regime in the calculation, and Figure 9 shows the calculation error according to the flow regime. In the UW experiment, the overall heat transfer coefficient was under-predicted owing to the difference in heat transfer in the entrance region. In the case of the modified RELAP5, the condensation heat transfer prediction was improved, compared with that of the original RELAP5.

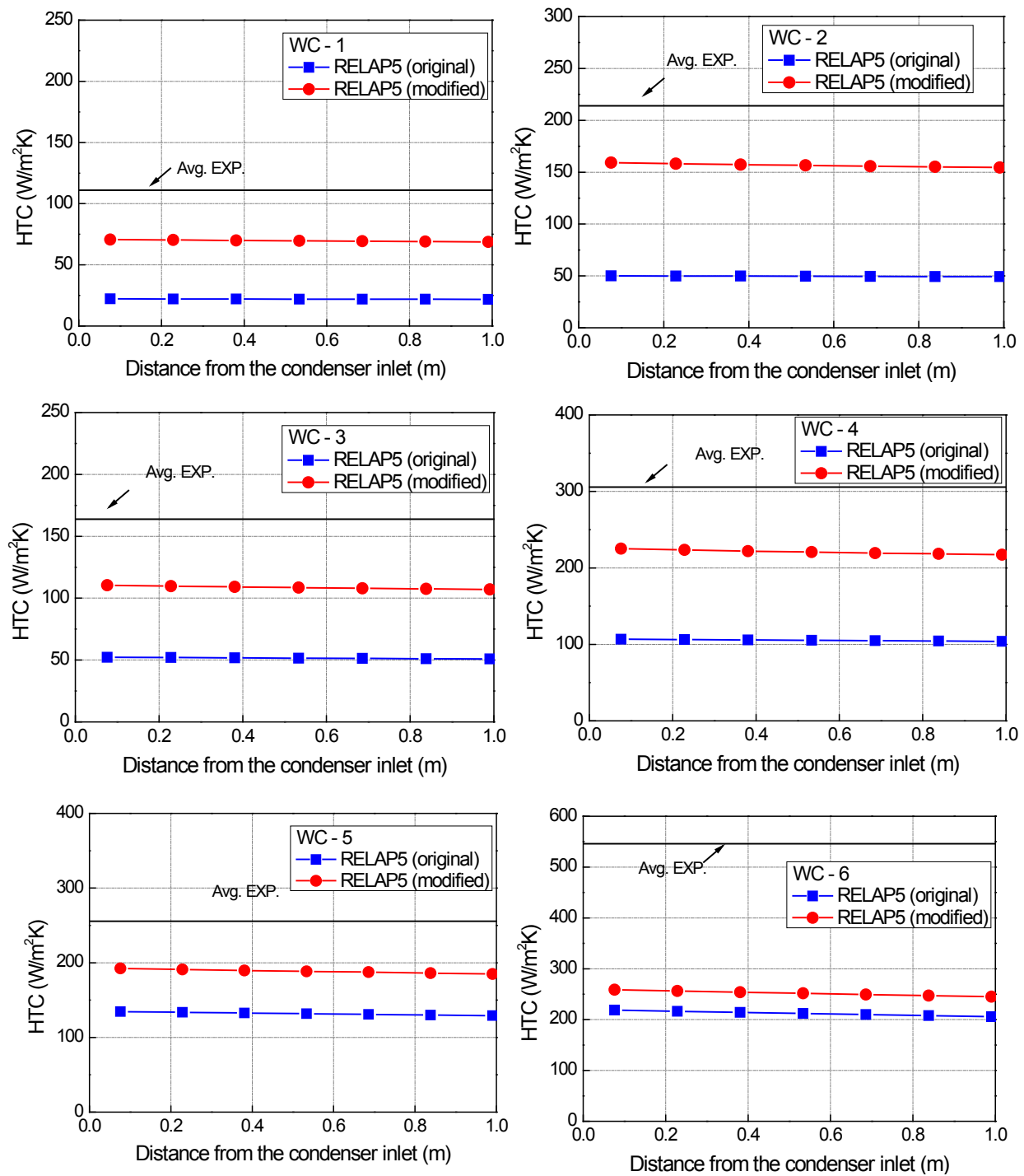


Figure 8 UW Calculation Results (RELAP5)

Table 5 Flow Regime of the UW Calculation

Test #	Forced convection turbulent flow	Natural convection flow
1		O
2	O	
3		O
4	O	
5		O
6		O

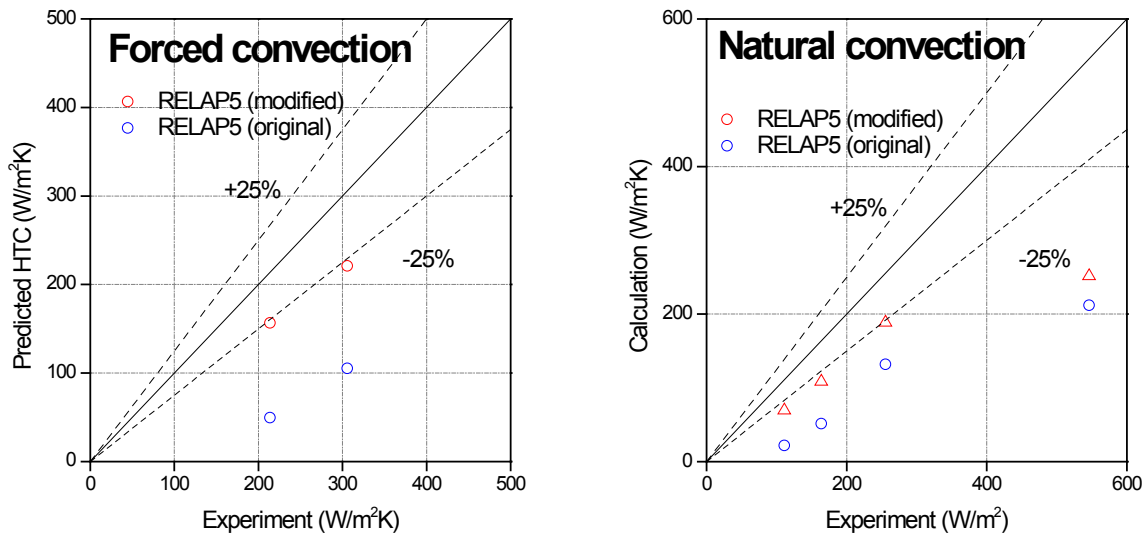


Figure 9 Comparison of the UW Experimental and Calculated Results

3.3 Analysis of the CONAN Experiment

The CONAN condensation experiment (Ref. 11) was analyzed using RELAP5 to verify the prediction performance for rectangular channel condensation experiments in a way similar to that in the previous two assessments. The experimental conditions and apparatus schematic are presented in Table 6 and Figure 10.

Table 6 CONAN Experimental Conditions

	Gas inlet condition			Cooling water inlet condition		
	Velocity	Inlet temperature	Air mass fraction	Inlet temperature	Outlet temperature	Mass flow rate
	(m/s)	(°C)	-	(°C)	(°C)	(kg/s)
P10-T30-V25	2.57	75.6	0.716	30.4	31.6	1.30
P15-T30-V25	2.60	83.5	0.581	29.6	31.4	1.31
P20-T30-V25	2.59	91.5	0.370	30.7	33.8	1.31
P25-T30-V25	2.60	93.8	0.290	31.1	34.8	1.30
P30-T30-V25	2.62	97.0	0.155	34.8	39.4	1.30
P10-T40-V25	2.58	79.8	0.651	40.3	41.3	1.78
P15-T40-V25	2.48	85.4	0.539	39.0	40.4	1.79
P20-T40-V25	2.59	89.5	0.432	40.0	41.9	1.77
P25-T40-V25	2.61	95.4	0.226	39.4	42.3	1.65
P30-T40-V25	2.63	97.5	0.132	42.3	46.9	1.28

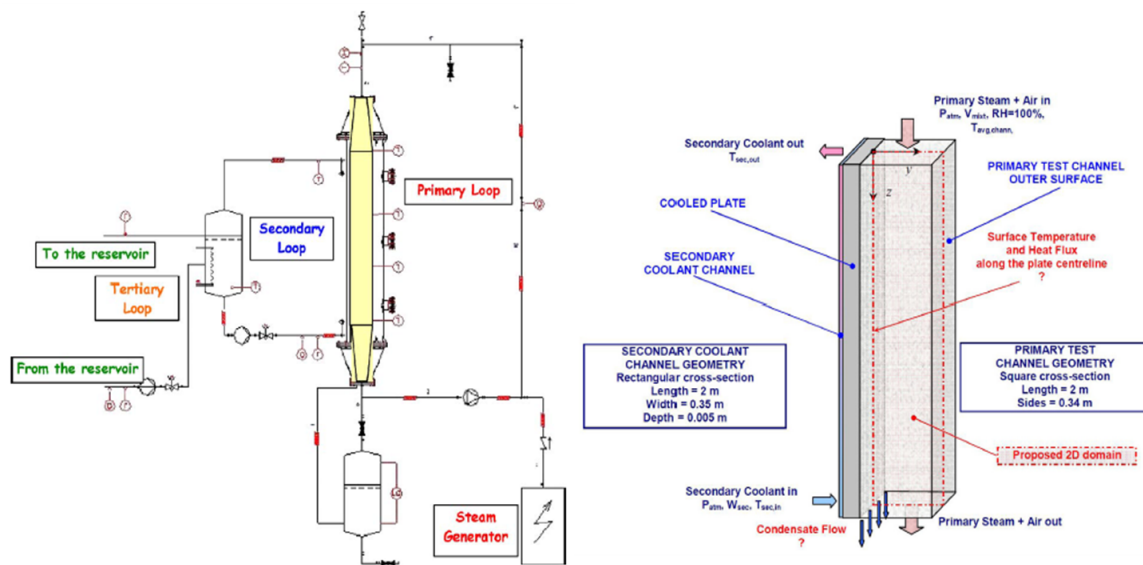


Figure 10 Schematic Diagram of the CONAN Experiment (Ref. 11)

For the RELAP5 calculation, the calculation node of the CONAN experiment was constructed as shown in Figure 11. In the figure, the gas mixture was injected from the time dependent volume-100 located at the top of pipe-300. The gas mixture then passed through time dependent junction-150 and then entered pipe-300, where condensation occurred. Pipe-300 has 8 volumes for the gas mixture flow, and heat exchange occurred through the pipe wall. The gas mixture then flowed out in a time dependent volume-500. The heat exchanger was simulated using the heat structure H-300, and the heat exchanger maintained the same constant temperature as in the experimental conditions.

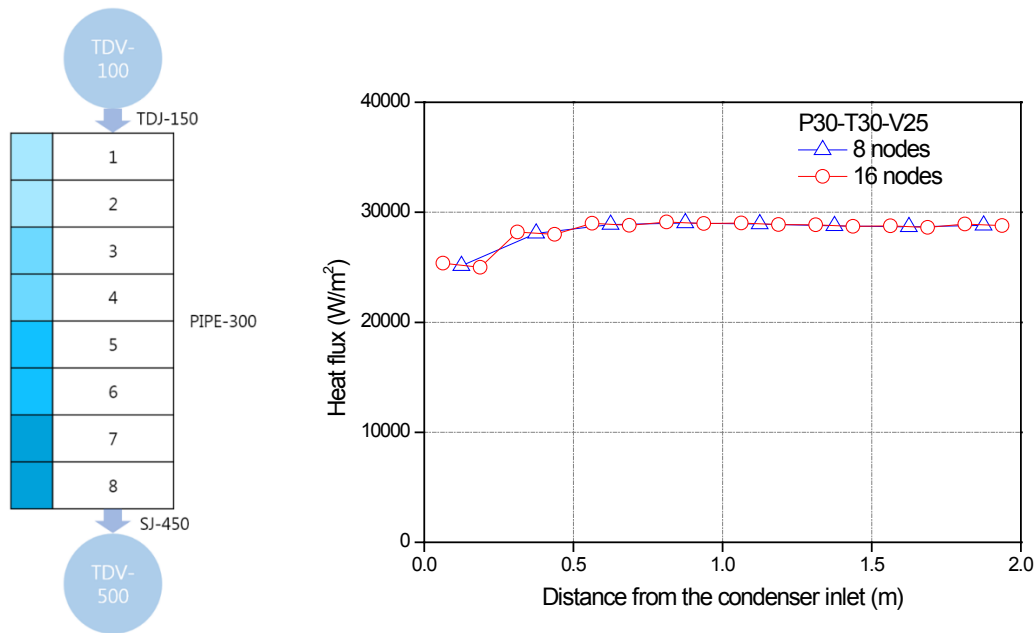


Figure 11 Results of the CONAN Simulation Nodalization and Node Convergence

Figure 12 shows the results of the analysis using the original and modified RELAP5. As shown in Figure 12, the original code under-estimates the condensation rate and the wall heat flux. After modification of the wall-film condensation model, the condensation heat flux of the RELAP5 increased, and the difference from the experimental result was reduced.

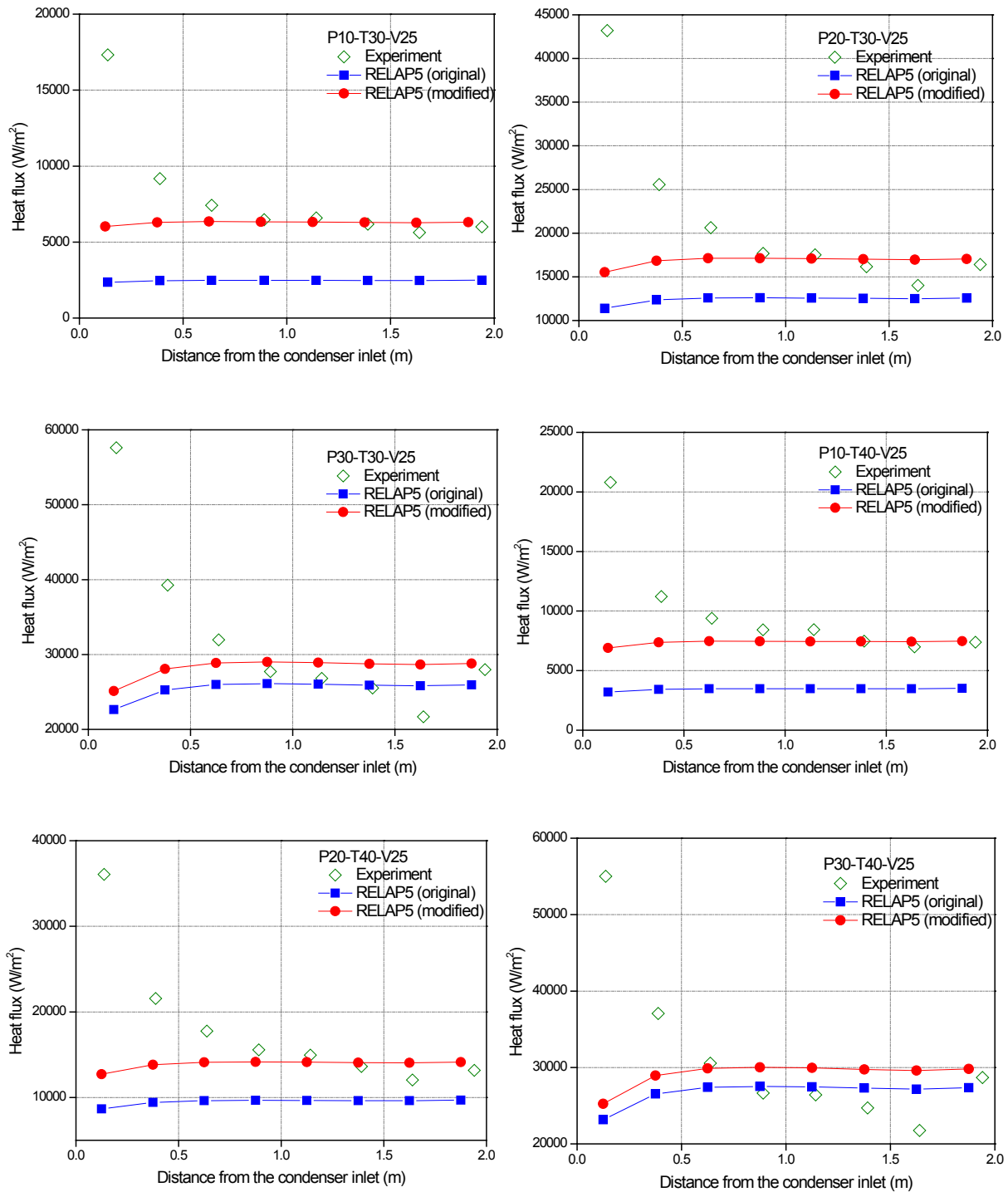


Figure 12 CONAN Calculation Results (RELAP5)

In Figure 13, the experimental and calculated results are compared with each other. The modified RELAP5 was used to analyze the condensation heat transfer within 20% (error) excluding the inlet region ($L/D < 1.2$), as shown in the figure. In the case of the CONAN experiment, all the experiments were in the forced-convection turbulent flow region.

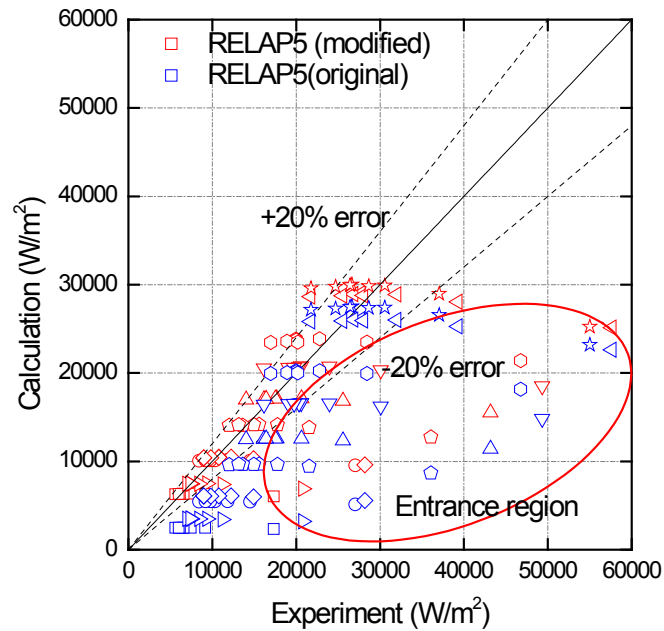


Figure 13 Results of the CONAN Experimental and Calculated Results

After assessing the calculation results of the plate condensation experiment through the three previous experiments, assessments of four additional experiments were conducted to evaluate the prediction performance of the condensation heat transfer on the tube inner wall.

3.4 Analysis of the MIT Experiments

The MIT condensation experiments (Ref. 12) were analyzed with RELAP5. The experimental conditions and experimental apparatus schematic are presented in Table 7 and Figure 14.

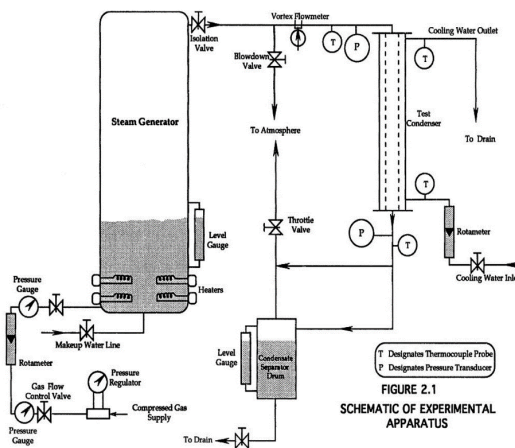


Figure 14 Schematic Diagram of the MIT Experiment (Ref. 12)

Table 7 MIT Experimental Conditions

Run No.	Gas temperature (°C)	Air mass fraction	Run No.	Gas temperature (°C)	Air mass fraction
1	100.0	0.09	27	119.9	0.27
2	100.0	0.15	28	119.9	0.31
3	100.2	0.18	29	119.9	0.36
4	100.0	0.24	30	140.0	0.10
5	100.1	0.29	31	140.2	0.15
6	100.0	0.33	32	140.2	0.20
7	119.9	0.08	33	140.0	0.25
8	119.9	0.14	34	140.0	0.32
9	119.9	0.19	35	100.0	0.11
10	119.6	0.26	36	100.5	0.14
11	120.0	0.33	37	100.5	0.19
12	119.9	0.42	38	100.5	0.24
13	140.0	0.11	39	100.5	0.30
14	139.9	0.18	40	100.5	0.35
15	139.9	0.24	41	120.1	0.10
16	139.9	0.30	42	120.1	0.15
17	139.9	0.34	43	120.1	0.20
18	100.0	0.12	44	120.1	0.24
19	100.1	0.17	45	120.1	0.31
20	100.2	0.21	46	120.1	0.34
21	100.2	0.25	47	140.0	0.10
22	100.0	0.31	48	140.0	0.15
23	100.0	0.35	49	140.0	0.20
24	120.0	0.11	50	140.1	0.25
25	120.0	0.15	51	140.1	0.30
26	119.9	0.22	52	140.1	0.35

For the simulation, the calculation node of the MIT experiment was constructed as shown in Figure 15. In the case of the tube type experiment, the wall temperature greatly influenced the heat flux calculation. For this reason, the calculation node for the MIT experiment was generated to match the temperature measurement points with the volume center locations. In the figure, the gas mixture was injected from the time dependent volume-100 located at the top of pipe-140. The gas mixture passed through the time dependent junction-105, and then entered pipe-140, where condensation occurred. Pipe-140 had 9 volumes for gas mixture flow, and heat exchange occurred through the pipe wall. The gas mixture then flowed out in time dependent volume-150. The heat exchanger was simulated using the heat structure H-140, and the heat exchanger maintained the temperature as in the experimental conditions.

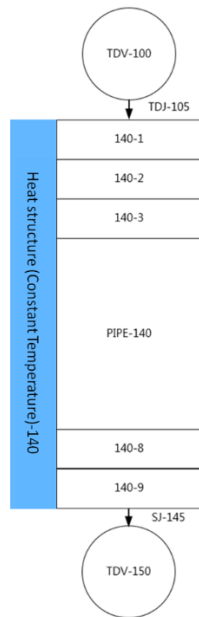


Figure 15 MIT Simulation Nodalization

Figure 16 shows the analysis results using the original and modified RELAP5. As shown in Figure 16, the original RELAP5 under-estimates the condensation rate and under-predicts the wall heat flux. After modification of the wall-film condensation model, the condensation heat flux of the RELAP5 increased, and the difference from the experimental result was reduced. The increase in heat flux was small because the non-condensable gas fraction was smaller than that of the previously analyzed plate wall experiments.

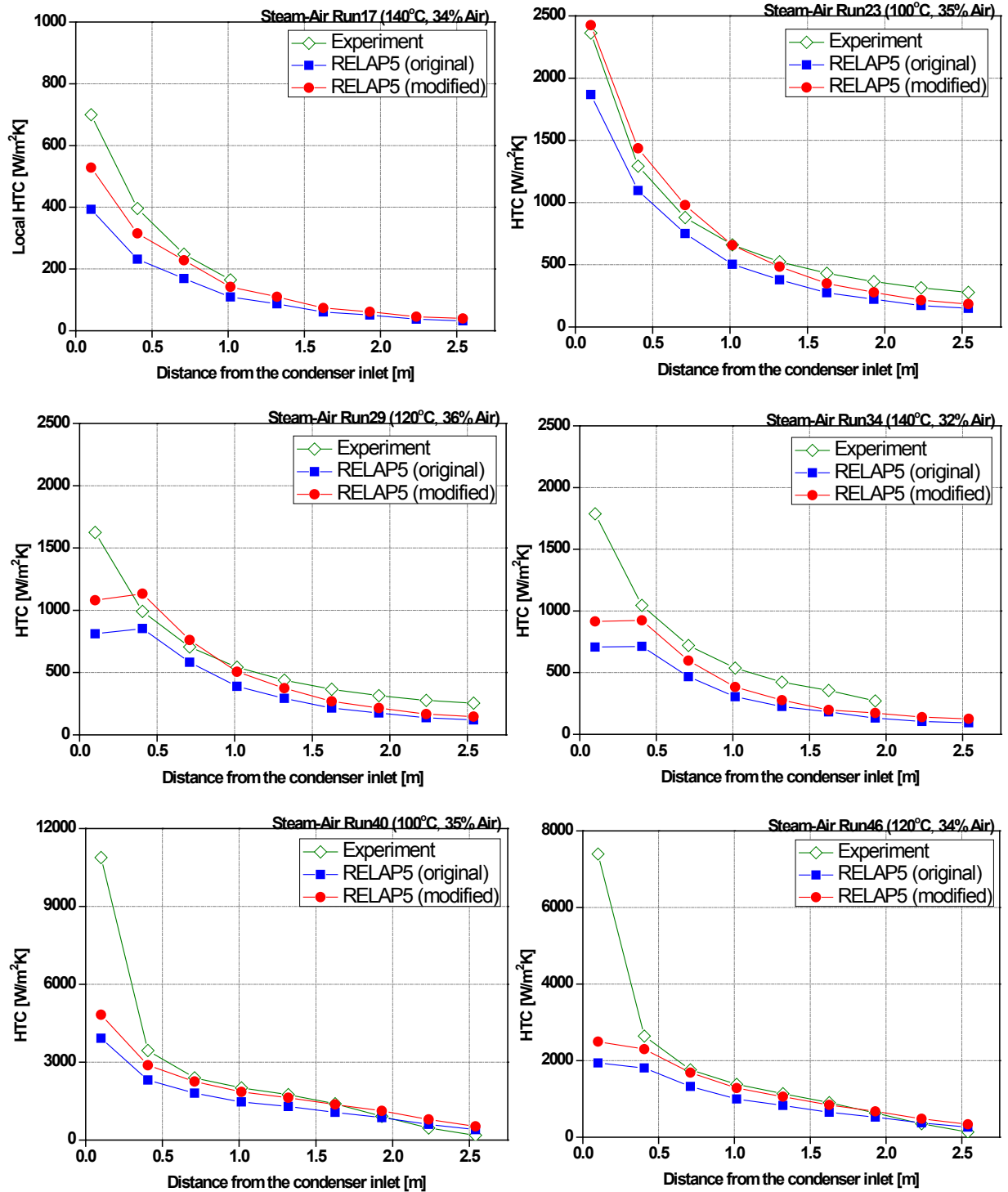


Figure 16 MIT Calculation Results (RELAP5)

Table 8 presents the flow regime in the calculation, and Figure 17 shows the error according to the flow regime. As shown in the figure, the results of the condensation heat flux of the modified RELAP5 were increased, compared with those of the original results, and accordingly, the error with the experiment was decreased. However, the analysis results were under-estimated under the natural-convection conditions. This may have originated from the relatively large uncertainties of the mass transfer coefficient model (Churchill and Chu, Ref. 13) used for natural convection. It seems necessary to improve the natural-convection heat transfer model of RELAP5 in the future for better prediction of the condensation heat transfer.

Table 8 Flow Regime of the MIT Calculation

Test #	Forced Convection turbulent flow	Natural convection flow
Run01~06	O	
Run07~17		O
Run18~52	O	

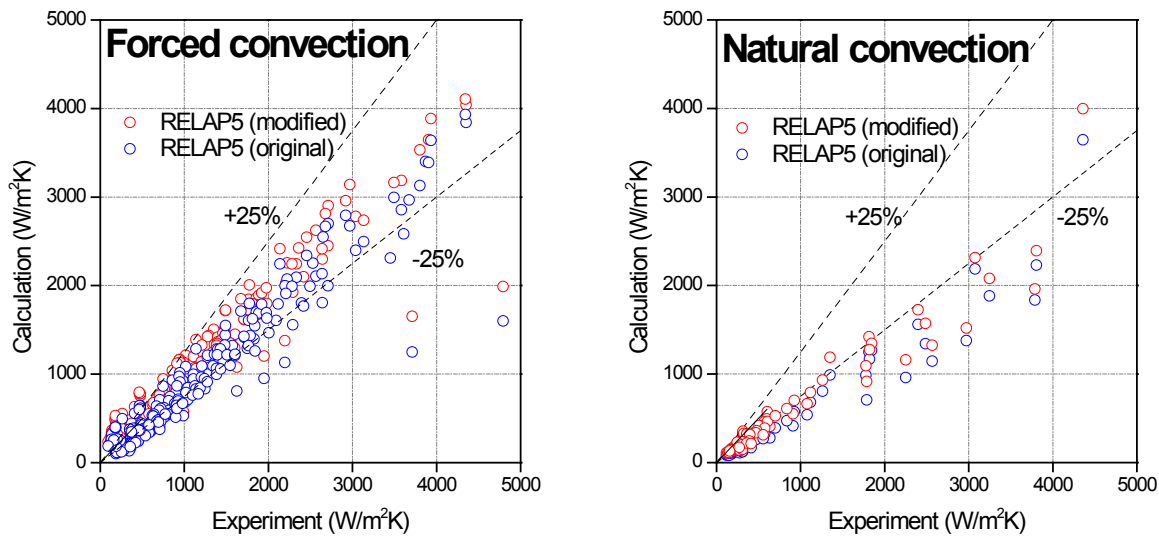


Figure 17 Comparison of the MIT Experimental and Calculated Results (RELAP5)

3.5 Analysis of the KAIST Experiment

The KAIST condensation experiments (Ref. 13) were analyzed using RELAP5. The experimental conditions and apparatus schematic are presented in Table 9 and Figure 18.

Table 9 KAIST Experimental Conditions

	Gas Temperature (°C)	Air mass fraction	Steam mass flow rate (kg/h)	Air mass flow rate (kg/h)
E13b	110.5	0.303	18.2	7.8
E11d	121.4	0.200	21.3	5.2
E4d	129.0	0.102	32.8	3.7
E12b	143.4	0.215	32.7	8.8

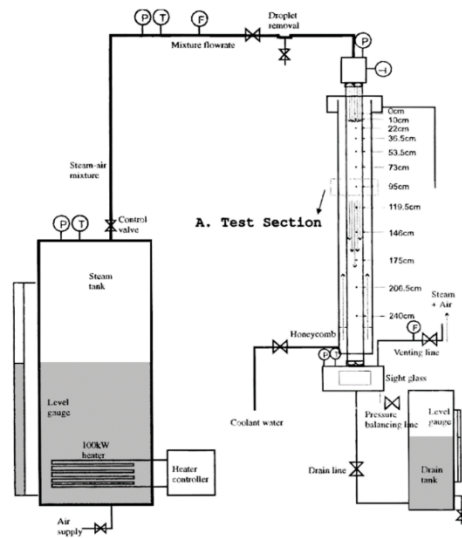


Figure 18 Schematic Diagram of the KAIST Experiment (Ref. 13)

For the RELAP5 calculation, the calculation node of the KAIST experiment was constructed as shown in Figure 19. In the case of the tube type experiment, the wall temperature vastly influenced the heat flux calculation. Therefore, the calculation node for the KAIST experiment was generated to match the temperature measurement points with the volume center locations. As shown in the figure, the gas mixture was injected from the time dependent volume-100 located at the top of pipe-140. The gas mixture passed through pipe-115, and then entered pipe-140, where condensation occurred. Pipe-140 had 13 volumes for the gas mixture flow, and condensation occurred on the pipe wall. Then, the gas mixture flowed out to the time dependent volume-180 through pipe-150. The heat exchanger was simulated using the heat structure H-140, and the temperature boundary condition was set as the experimental wall temperature, summarized in Ref. 13.

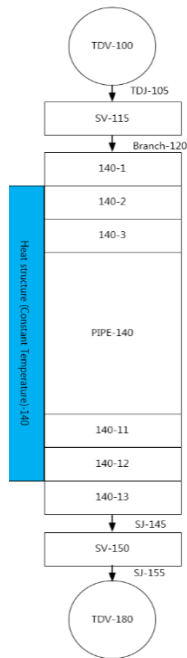


Figure 19 KAIST Simulation Nodalization

Figure 20 shows the analysis results using the original and modified RELAP5. As shown in Figure 20, the heat flux results of the modified RELAP5 at the inlet region were improved. Meanwhile, the KAIST test simulation showed that the increase in heat flux was small because the non-condensable gas fraction was smaller than that of the previously analyzed plate wall experiments.

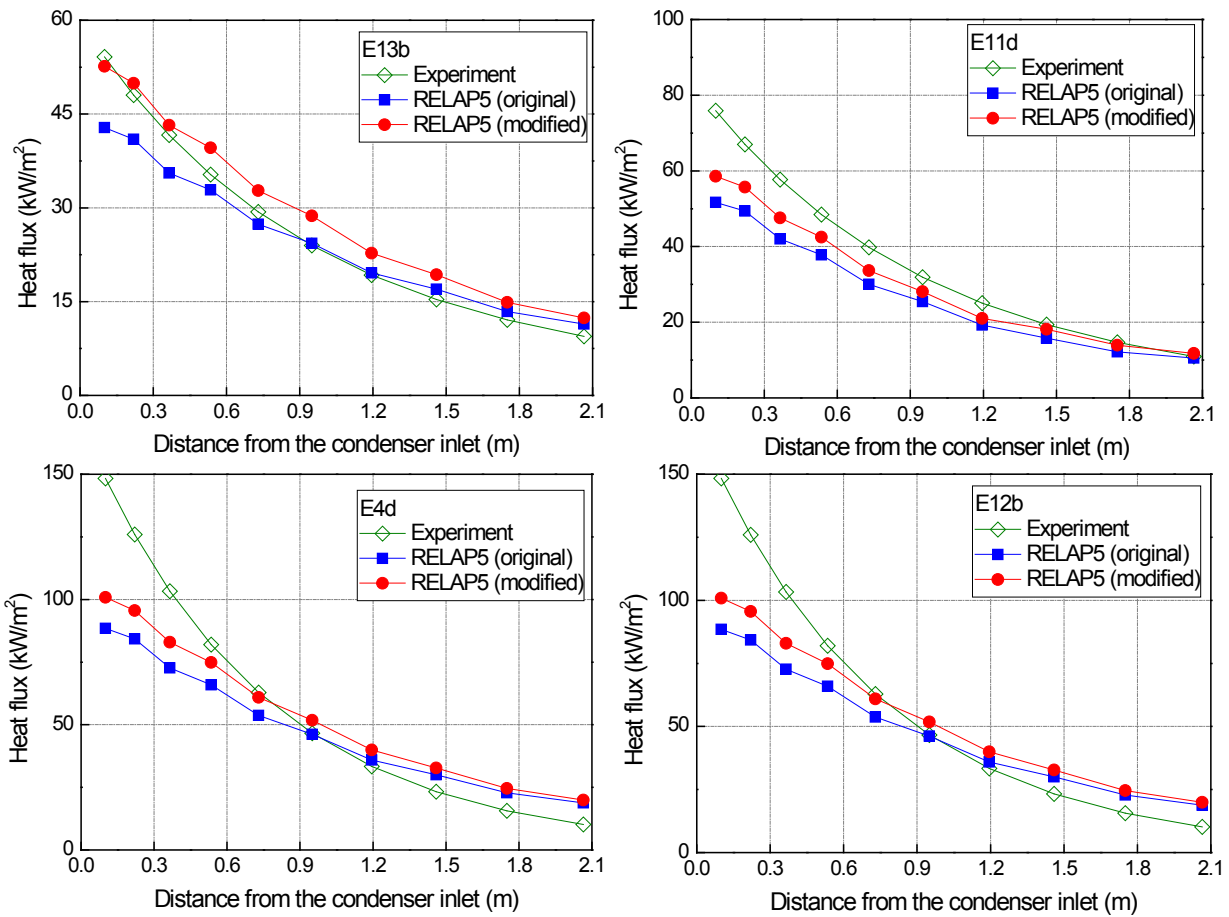


Figure 20 KAIST Calculation Results (RELAP5)

Table 10 presents the flow regime in the calculation, and Figure 21 shows the error according to the flow regime. As shown in the figure, the results of the condensation heat flux of the modified RELAP5 was increased when compared with the original RELAP5 results, and accordingly, the difference from the experiment was decreased. On the other hand, the heat results were over-estimated mainly under natural-convection conditions. This is opposite to the results of the MIT experiment calculations with which RELAP showed under-prediction and thus, further validation and improvement seem necessary for the natural-convection condensation heat transfer model.

Table 10 Flow Regime of the KAIST Calculation

Test #	Forced convection turbulent flow	Natural convection flow
E13b	O	
E11d	O	O
E4d	O	O
E12b	O	

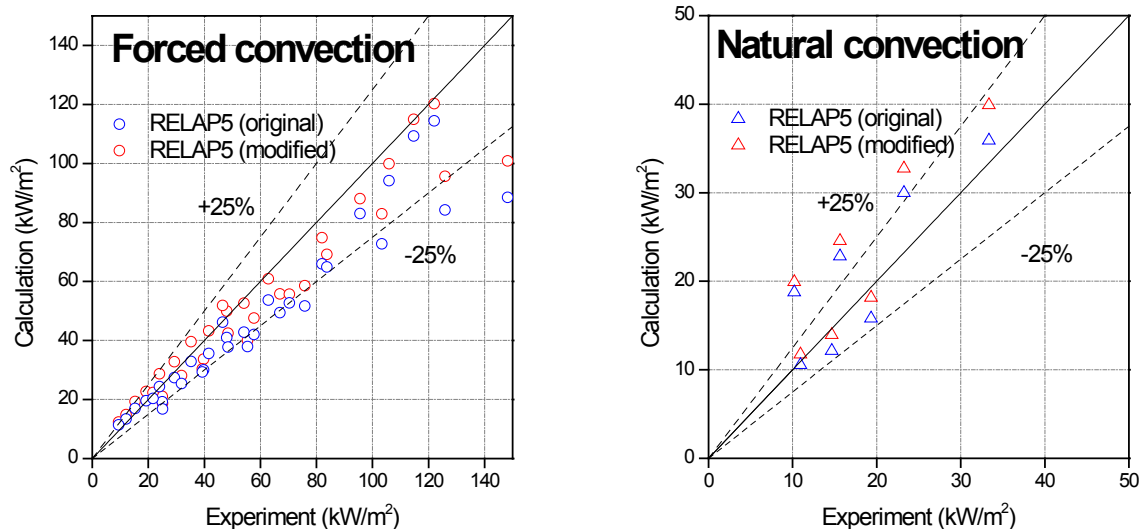


Figure 21 Comparison of the KAIST Experimental and Calculated Results

3.6 Analysis of the POSTECH Experiment

The POSTECH condensation experiments (Ref. 14) were analyzed using RELAP5. The experimental conditions and apparatus schematic are presented in Table 11 and Figure 22.

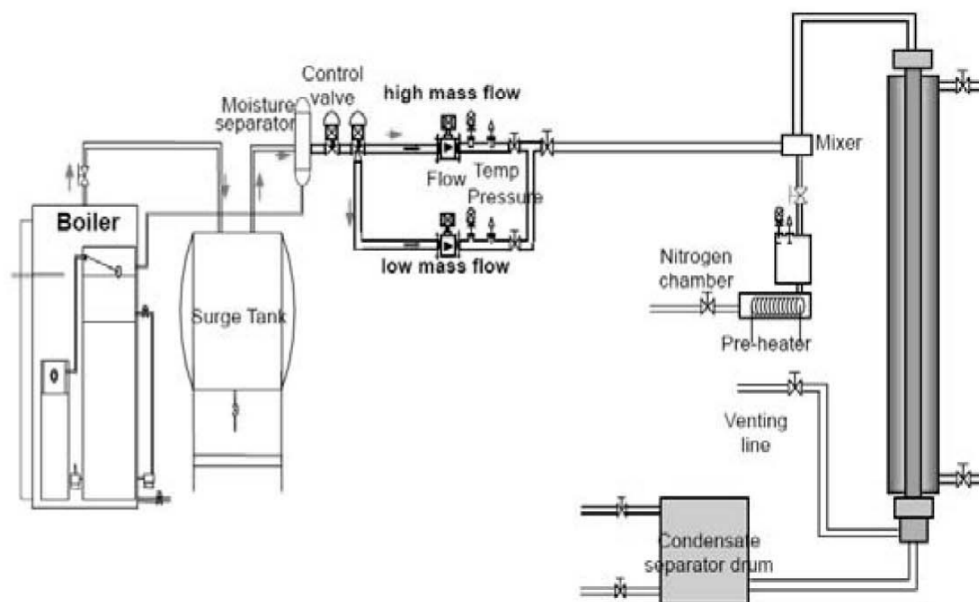


Figure 22 Schematic Diagram of the POSTECH Experiment (Ref. 14)

Table 11 POSTECH Experimental Conditions

Run No.	Gas inlet temperature (°C)	Outlet pressure (kPa)	Steam mass flow rate (kg/h)	Air mass flow rate (kg/h)
MB 11	99.91	103.75	6.53	0.23
MB 12	98.19	104.78	6.52	0.73
MB 13	96.49	106.26	6.51	1.65
MB 14	94.05	107.94	6.50	2.81
MB 15	91.98	111.71	6.53	4.37
MB 21	99.45	103.84	8.56	0.26
MB 22	98.22	104.91	8.56	0.97
MB 23	96.80	106.91	8.56	2.17
MB 24	95.27	110.61	8.57	3.67
MB 25	93.97	117.76	8.53	5.72
MB 31	99.36	103.77	11.19	0.35
MB 32	98.52	105.51	11.22	1.28
MB 33	97.58	109.41	11.22	2.82
MB 34	96.94	116.00	11.18	4.80
MB 41	99.53	104.05	13.79	0.43
MB 42	98.93	106.38	13.75	1.56
MB 43	98.51	113.16	13.74	3.57
MB 44	99.14	124.03	13.78	5.97
MB 51	99.68	104.55	16.03	0.51
MB 52	99.35	107.62	15.99	1.79
MB 53	99.79	117.10	16.05	4.04
MB 61	99.81	104.95	18.41	0.58
MB 62	100.24	110.33	18.45	2.06
MB 63	101.81	125.02	18.51	4.67
MB 71	100.67	107.60	21.86	0.69
MB 72	102.27	118.13	22.35	2.48
MB 81	102.76	115.60	28.14	0.88
MB 82	105.10	130.51	26.86	3.20

For the calculation, the nodalization of the POSTECH experiment was constructed as shown in Figure 23. In the case of the tube type experiment, the wall temperature greatly influenced the heat flux calculation. For this reason, the calculation node for the POSTECH experiment was generated to match the temperature measurement points with the volume center locations. As shown in the figure, the gas mixture was injected from the time dependent volume-100 located at the top of pipe-140. The gas mixture passed through the time dependent junction-105, and then entered pipe-140, where condensation occurred. Pipe-140 had 13 volumes for the gas mixture flow, and heat exchange occurred through the pipe wall. The gas mixture then flowed out in time

dependent volume-180. The heat exchanger was simulated using the heat structure H-140, and the temperature boundary condition was set as the experimental wall temperature, summarized in Ref. 14.

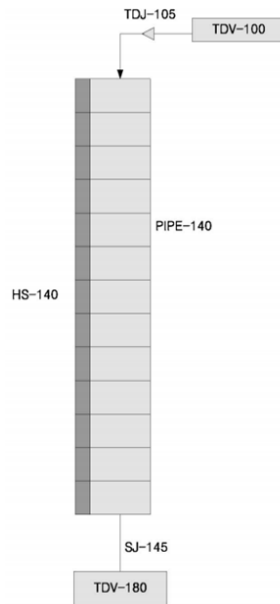


Figure 23 POSTECH Simulation Nodalization

Figure 24 shows the analysis results using the original and modified RELAP5. As shown in Figure 24, the heat flux results of the modified RELAP5 at the inlet region were improved. The increase in heat flux was relatively small because the non-condensable gas fraction was small compared with that in the plate wall experiment analyzed previously. Meanwhile, the calculation with the large steam flow rate showed a large error in the inlet region. It is considered that the error is caused by the uncertainties in the experiment for that region and is a deficiency of the condensation model for the inlet region. The upper wall surface temperature of the condenser was very close to the gas temperature in the experiment. Therefore, the heat transfer coefficient in the experiment, which is calculated based on the wall and gas temperature difference and the heat flux evaluated from the enthalpy rise in the cooling jacket, was estimated as very large for that region. Using the condensation model in RELAP, such a high heat transfer coefficient cannot be predicted and the predicted heat flux was significantly under-predicted. This is because the wall temperature in the experimental result was used as the boundary condition in the calculation. Because the wall temperature became considerably lower than the gas temperature, the calculated heat flux reasonably captured the experimental results.

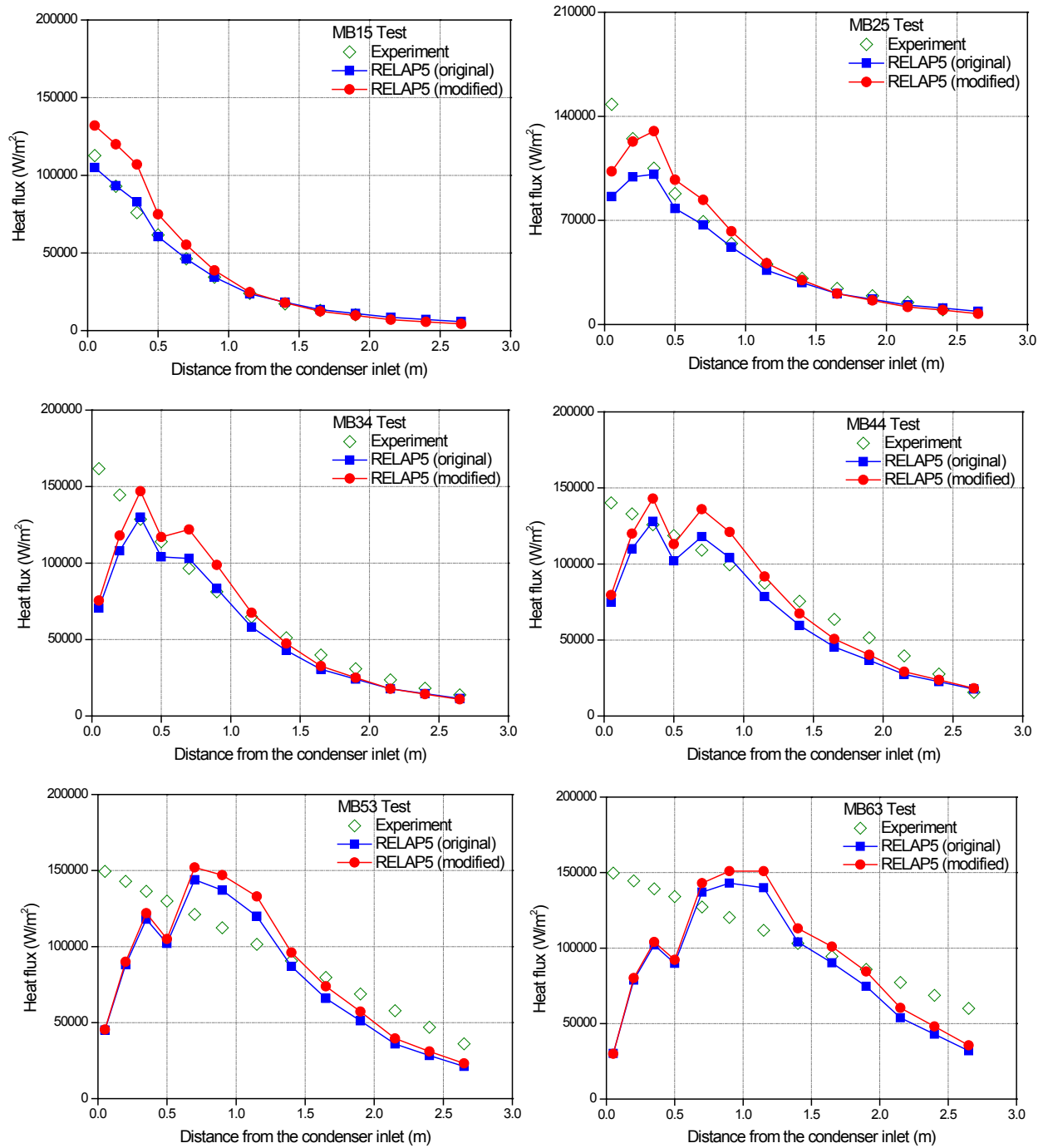


Figure 24 POSTECH Calculation Results (RELAP5)

Figure 25 shows the error in the calculation according to the flow regime. In the case of the POSTECH experiment, all experiments were in the forced-convection turbulent flow region. When it was compared to the experiment results, as shown in the figure, the result of condensation heat flux of the modified RELAP5 increased, and accordingly, the error with the

experiment decreased. The heat flux of the modified RELAP5 could be predicted by an error of approximately 40% in the region, except at the inlet.

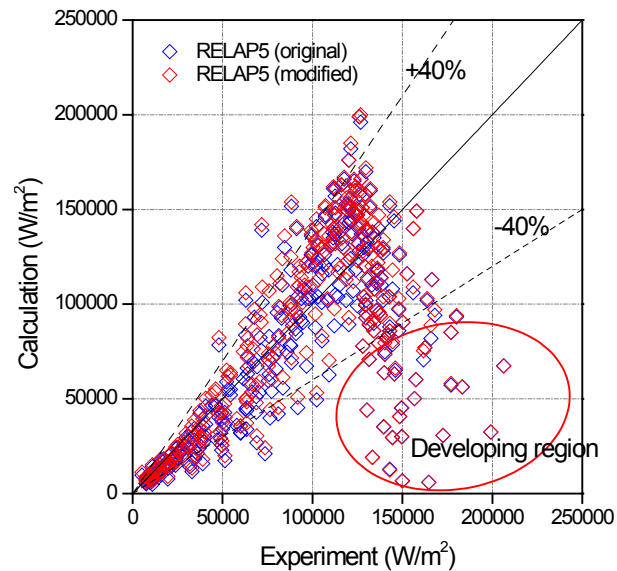


Figure 25 Comparison of POSTECH Experimental and Calculated Results (RELAP5)

3.7 Analysis of the UCB Experiments

The UCB condensation experiments (Ref. 10) were analyzed using RELAP5. The experimental conditions and apparatus schematic are presented in Table 12 and Figure 26.

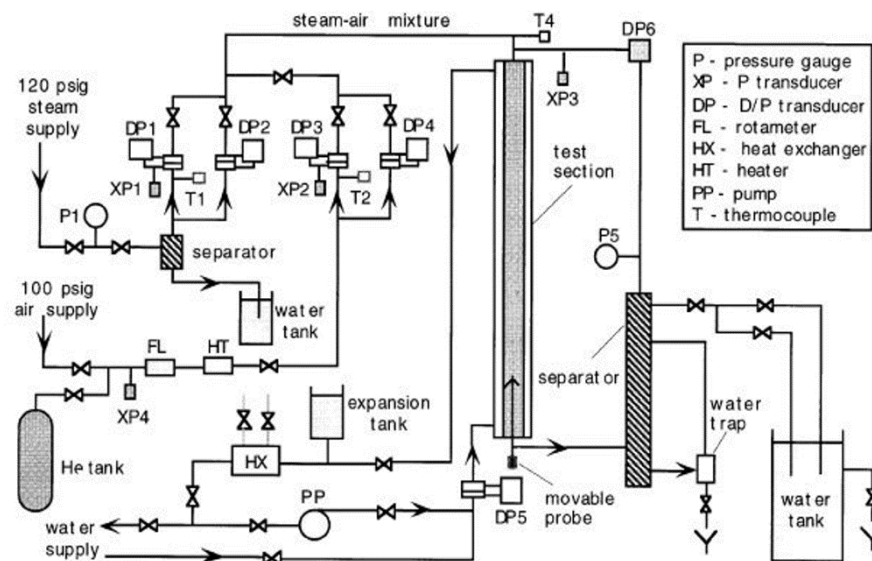


Figure 26 Schematic Diagram of the UCB Experiment (Ref. 10)

Table 12 UCB Experimental Conditions

Run No.	Gas inlet temperature (°C)	Pressure (bar)	Steam mass flow rate (kg/hr)	Air mass fraction
2.1-1	143.39	4	50	0.01
2.1-4	142.69	4	50	0.04
2.1-7	141.22	4	50	0.10
2.1-9	138.47	4	60	0.20
2.1-13	131.52	4	50	0.40
3.2-3	132.43	3	60	0.05
3.2-4	142.45	4	60	0.05
3.3-3	131.26	3	60	0.10
3.3-4	141.22	4	60	0.10
3.4-2	115.70	2	60	0.20
3.4-3	128.66	3	60	0.20
3.5-3	122.07	3	60	0.40
3.5-4	133.48	4	60	0.35
4.2-2	119.20	2	30	0.05
4.2-3	132.43	3	30	0.05
4.3-2	118.11	2	30	0.10
4.3-3	131.26	3	30	0.10
4.4-2	116.46	2	36	0.17
4.4-3	128.66	3	30	0.20
4.5-2	109.58	2	30	0.40
4.5-3	122.07	3	30	0.40

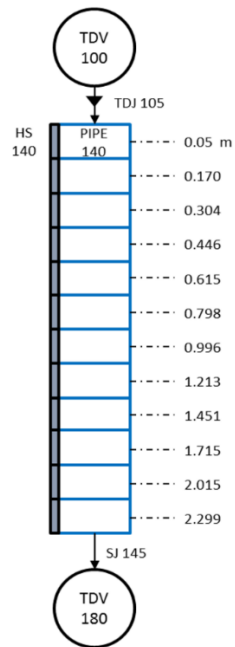


Figure 27 UCB Simulation Nodalization

For the RELAP5 calculation, the nodalization of UCB experiment was constructed as shown in Figure 27. In the case of the tube type experiment, the wall temperature greatly influenced the heat flux calculation. For this reason, the calculation node for the UCB experiment was generated to match the temperature measurement points with the volume center locations. In the figure, the gas mixture was injected from the time dependent volume-100 located at the top of pipe-140. The gas mixture passed through the time dependent junction-105, and then entered pipe-140, where condensation occurred. Pipe-140 had 12 volumes for the gas mixture flow, and heat exchange occurred through the pipe wall. The gas mixture then flowed out in a time dependent volume-180. The heat exchanger was simulated using the heat structure H-140, and the temperature boundary condition was set as the experimental wall temperature, as summarized in Ref. 10.

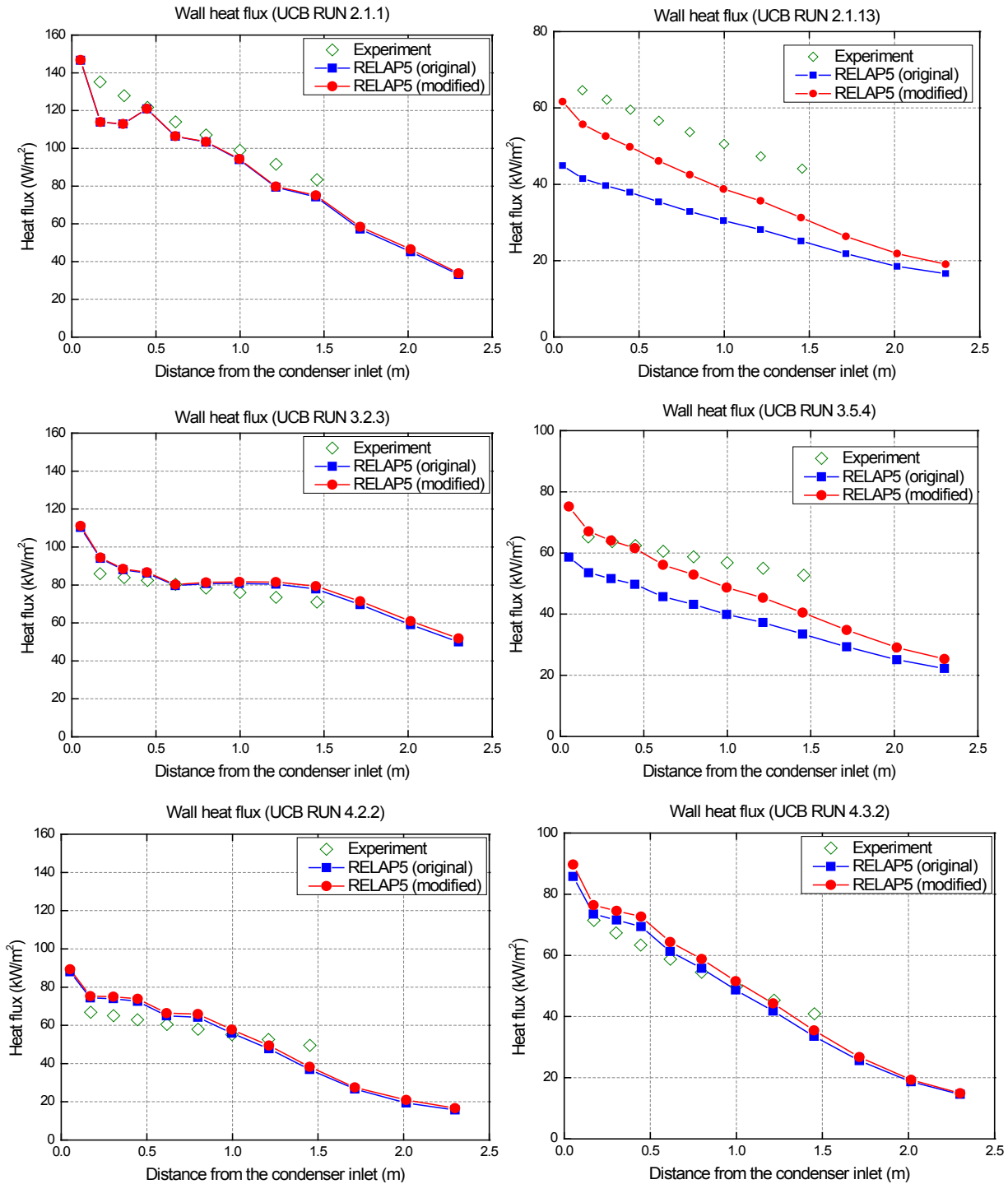


Figure 28 UCB Calculation Results

Figure 28 shows the result of the analysis using the original and modified RELAP5. As shown in the figure, the heat flux of the modified RELAP5 increased compared with that of the original RELAP5. The increase of the heat flux was larger in the case of the experiment in which the fraction of non-condensable gas was large. However, in cases where a large fraction of non-

condensable gas was used, the condensation heat-flux was sometimes over-predicted in the calculation, and the error was even larger than that of the original RELAP5.

Figure 29 shows the calculation error according to the flow regime. In the case of the UCB experiment, all experiments were in the forced-convection turbulent flow region. When it was compared with the experimental results, as shown in the figure, the result of the condensation heat flux of the modified RELAP5 increased when compared with the original RELAP5 results, and accordingly, the error with the small non-condensable gas mass fraction experiments also decreased. However, as the condensation heat flux increased, the error became larger than that of the original RELAP5.

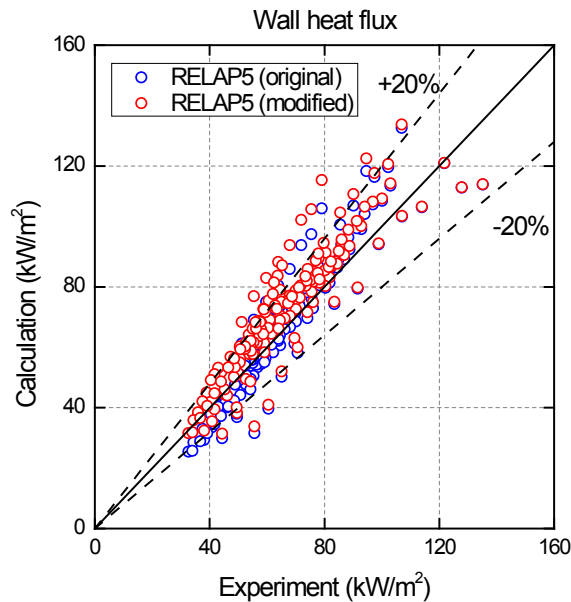


Figure 29 Comparison of UCB Experimental and Calculated Results

3.8 Synthesis of the Analysis Results

In this section, the experimental and calculated results were compared according to the flow regime. The flow regimes of all experiments were divided into forced-convection turbulent flow and natural-convection flow, according to the model in RELAP5. When the heat flux results were compared, the inlet region, in which the RELAP5 code does not adequately simulate the condensation heat transfer, was excluded from the comparison. The COPAIN, CONAN, KAIST, POSTECH, and UCB calculations were compared with the measured heat fluxes, and the UW and MIT calculations were compared with the measured heat transfer coefficients.

Figure 30 and Figure 31 show the comparison results of the heat flux and heat transfer coefficient for the forced-convection turbulent flow. As shown in the results, in general, the heat flux could be interpreted within a 30% error; however, the results were over-predicted in the high heat flux region. Figure 32 and Figure 33 show the results of heat flux and heat transfer coefficient with a natural-convection flow. As a result of the heat flux comparison, most of the results were found to be within 30% error; however, the comparison shows that the calculation results were under-predicted with respect to the heat transfer coefficient.

In conclusion, although the error in the condensation with a high non-condensable gas fraction was improved with the modified RELAP5, the condensation heat transfer rate is still over-predicted or under-predicted depending on the flow regime. Therefore, it is necessary to analyze the difference in the condensation according to the flow regime, and to improve the Colburn-Hougen model itself (or the mass transfer coefficient model, which has the most significant effect on the condensation heat transfer prediction), so that the condensation heat transfer predicted by RELAP5 can be improved.

In the case of the plate condensation experiments, the calculation results were greatly improved with the modified RELAP5. However, the plate experiments have larger hydraulic diameters and a clearer inlet effect; hence, the RELAP5 code under-predicts the condensation heat transfer at the inlet region, $L/D < 1.2$ (Figure 34). On the other hand, in the case of the pipe condensation experiment, the RELAP5 code did not under-predict the condensation heat transfer in the inlet region, because the hydraulic diameter of the pipe was relatively smaller than the pipe length, and the inlet effect was not distinct. Therefore, it is expected that if the model is improved to reflect the inlet effect in the large hydraulic diameter test, the accuracy of the code for evaluating the condensation heat transfer could be improved.

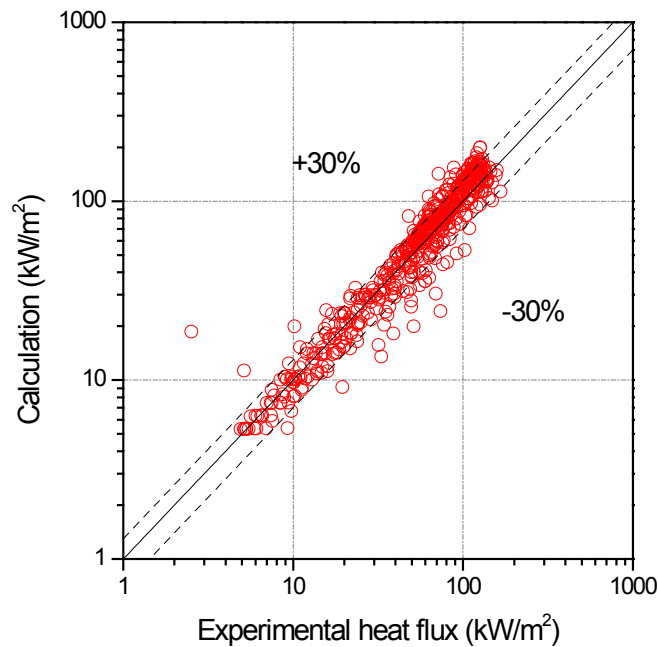


Figure 30 Heat Flux Comparison Results (Forced Convection)

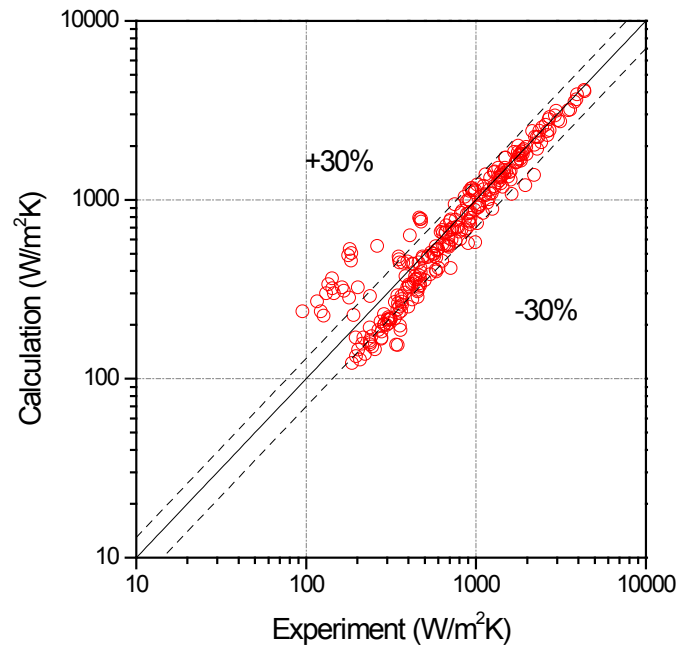


Figure 31 Heat Transfer Coefficient Comparison Results (Forced Convection)

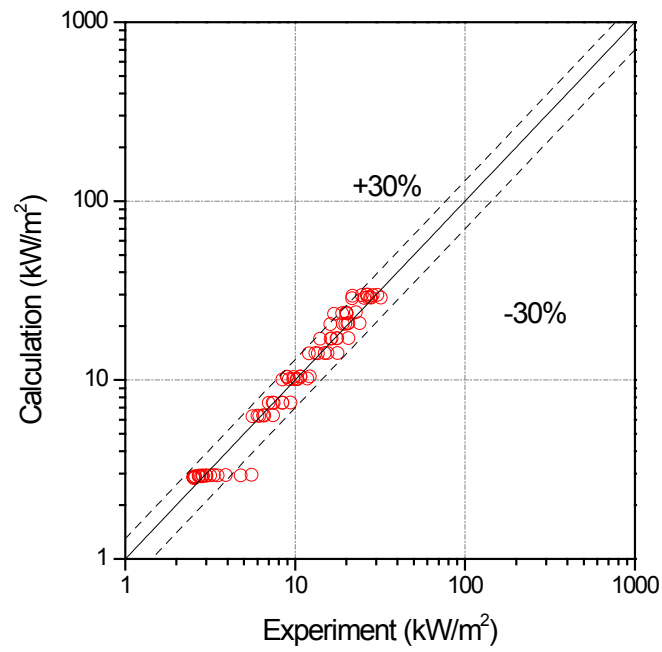


Figure 32 Heat Flux Comparison Results (Natural Convection)

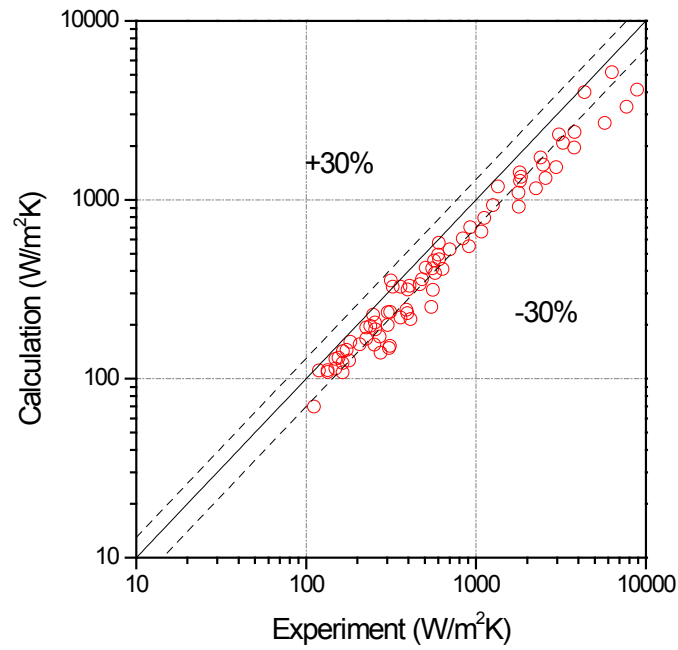


Figure 33 Heat Transfer Coefficient Results (Natural Convection)

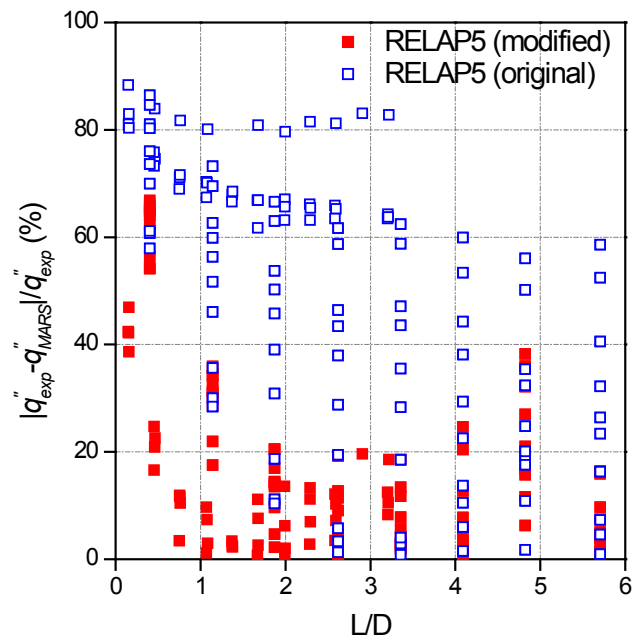


Figure 34 Plate Condensation Error: Experimental vs Simulation

4 TRACE ASSESSMENT RESULTS

For the film condensation calculation at the interface in the presence of non-condensable gases, TRACE uses the Kuhn model (Ref. 15). The Kuhn model calculates the heat transfer from the energy conservation equation at the liquid-gas interface. At this time, unlike in RELAP5, sensible heat between the gas and the interface is considered. The film condensation model of TRACE (TRACE V5p04, Ref. 3) is compared with RELAP5 as shown in Table 13 (the nomenclature of the equation in Ref. 3 was converted to follow that of RELAP5.).

Table 13 Film Condensation Model Comparison Between RELAP5 and TRACE

RELAP5	TRACE
Colburn-Hougen model	Kuhn model
$q'' = h_c (T_{vi} - T_w) = h_m \rho_{vb} \ln \left(\frac{1 - \frac{P_{vi}}{P}}{1 - \frac{P_{vb}}{P}} \right)$	$q'' = h_l (T_{vi} - T_l) = f_{fog} h_{conv} (T_g - T_l) + \Gamma'' h_{fg}$ $\Gamma'' = h_m \frac{\rho_{vb}}{X_{vb}} \ln \left(\frac{1 - X_{vi}}{1 - X_{vb}} \right)$
Mass transfer coefficient Laminar flow: Rohsenow-Choi (Ref. 5) Turbulent flow: Gilliland (Ref. 5) Natural convection: Churchill-Chu (Ref. 6)	Mass transfer coefficient Laminar flow: $Sh = 3.66$ Turbulent flow: Gnielinski (Ref. 16) Natural convection: McAdams (Ref. 17)

The condensation mass flux term of TRACE is presented below.

$$j_v = h_m \frac{\rho_{vb}}{X_{v,b}} \ln \left(\frac{1 - X_{v,i}}{1 - X_{v,b}} \right),$$

Where X_{vi} = mass fraction of steam at the liquid-gas-vapor interface, and

X_{vb} = mass fraction of steam at the bulk stream.

In the equation, the condensation mass flux of TRACE is determined by the difference between X_{vi} and X_{vb} . This definition is different from that in RELAP5, which uses the partial pressure difference between the interface and bulk stream. In addition to that, TRACE considers sensible heat transfer between the liquid and gas (which RELAP5 neglects), and uses a different mass transfer coefficient model from RELAP5. Especially under natural convection, RELAP5 uses the Churchill and Chu correlation, whereas TRACE uses the McAdams correlation. This generates a difference in the condensation simulation within the natural-convection regime.

In order to analyze quantitatively the difference between the condensation heat transfer model of RELAP5 and TRACE, the same experiments used in the RELAP5 assessment were

analyzed using TRACE. In analyzing the condensation heat transfer in the plate-type experiment, the non-physical behavior of the TRACE calculation results, with respect to the interface heat flux, appeared as shown in Figure 35, which is the COPAIN P0443 simulation result. In the other plate-type experimental analyses, a similar trend in the condensation heat flux was observed.

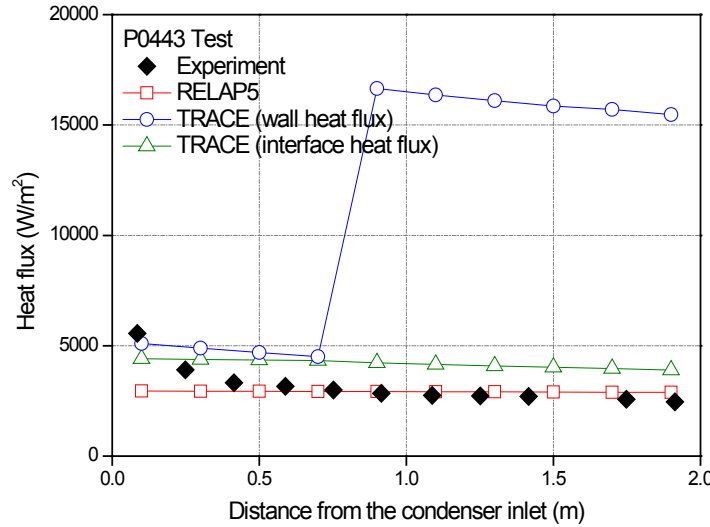


Figure 35 COPAIN P0443 Test TRACE Analysis Result (With Hydraulic Diameter)

In order to find the cause of the unphysical trend, the wall condensation heat transfer model of the TRACE code was analyzed and it was confirmed that TRACE calculates the wall heat flux and liquid film thickness using the following equations,

$$q'' = h_{wl} (T_l - T_w),$$

$$h_{wl} = \frac{k}{\delta} Nu_{wl},$$

$$\delta = \frac{D_h (1 - \sqrt{\alpha})}{2}.$$

Where h_{wl} = liquid film heat transfer coefficient (W/m²·k)

k = conductivity of liquid film (W/m·k)

δ = liquid film thickness (m)

D_h = Hydraulic diameter (m)

α = Void fraction

To calculate the liquid film thickness (δ) in the above equation, the TRACE code uses the hydrodynamic diameter instead of heated diameter, which was identified as the reason for the unphysical trend. In the plate wall condensation, those two diameters have different values and the heated diameter is the appropriate length scale for the liquid film thickness estimation. Even though TRACE allows the input of both the hydraulic and heated diameter, it uses the former for the liquid film thickness calculation. Thus, for proper prediction of the plate wall condensation, the heated diameter needs to be applied instead of the hydraulic diameter. Therefore, in the plate-type experiments, the heated diameter was used in the input data, and the problematic unphysical increase of condensation heat flux was resolved, as shown in Figure 37.

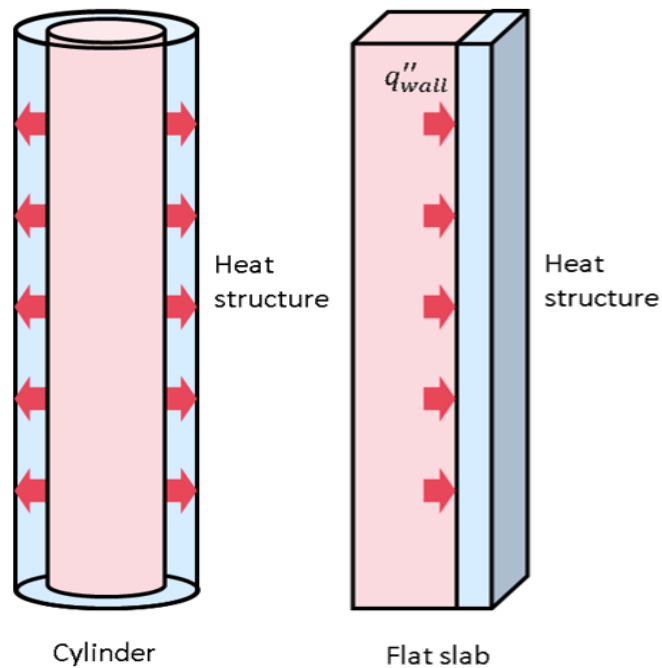


Figure 36 Schematic of Heated Length Calculation Method in Tube and Plate Wall

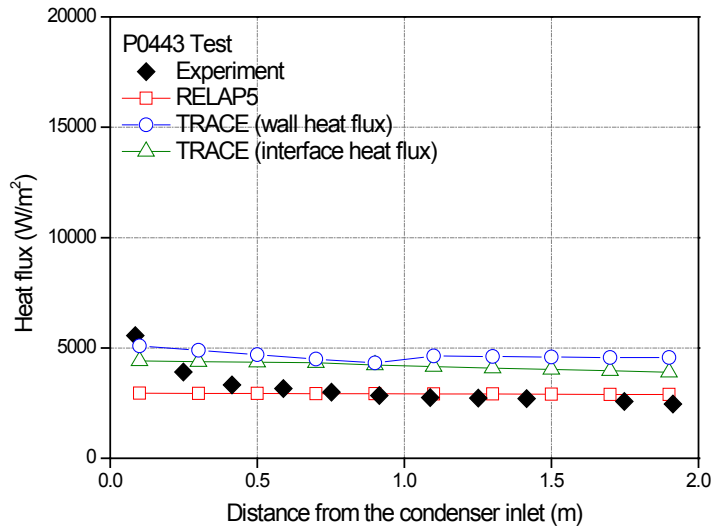


Figure 37 COPAIN P0443 Test TRACE Analysis Result (With Heated Diameter)

4.1 Analysis of the COPAIN Experiment

The analyses for the COPAIN P0441, P0443, P0444, and P0344 experiments were conducted in the same ways as for RELAP5. The experimental conditions and the schematic diagram of the experimental apparatus are presented in Table 2 and Figure 2, respectively, and the nodalization is the same as for RELAP5, as shown in Figure 3.

The analysis results of the COPAIN experiment using TRACE are shown in Figure 38, which shows condensed heat flux results of TRACE that are higher than those of RELAP5.

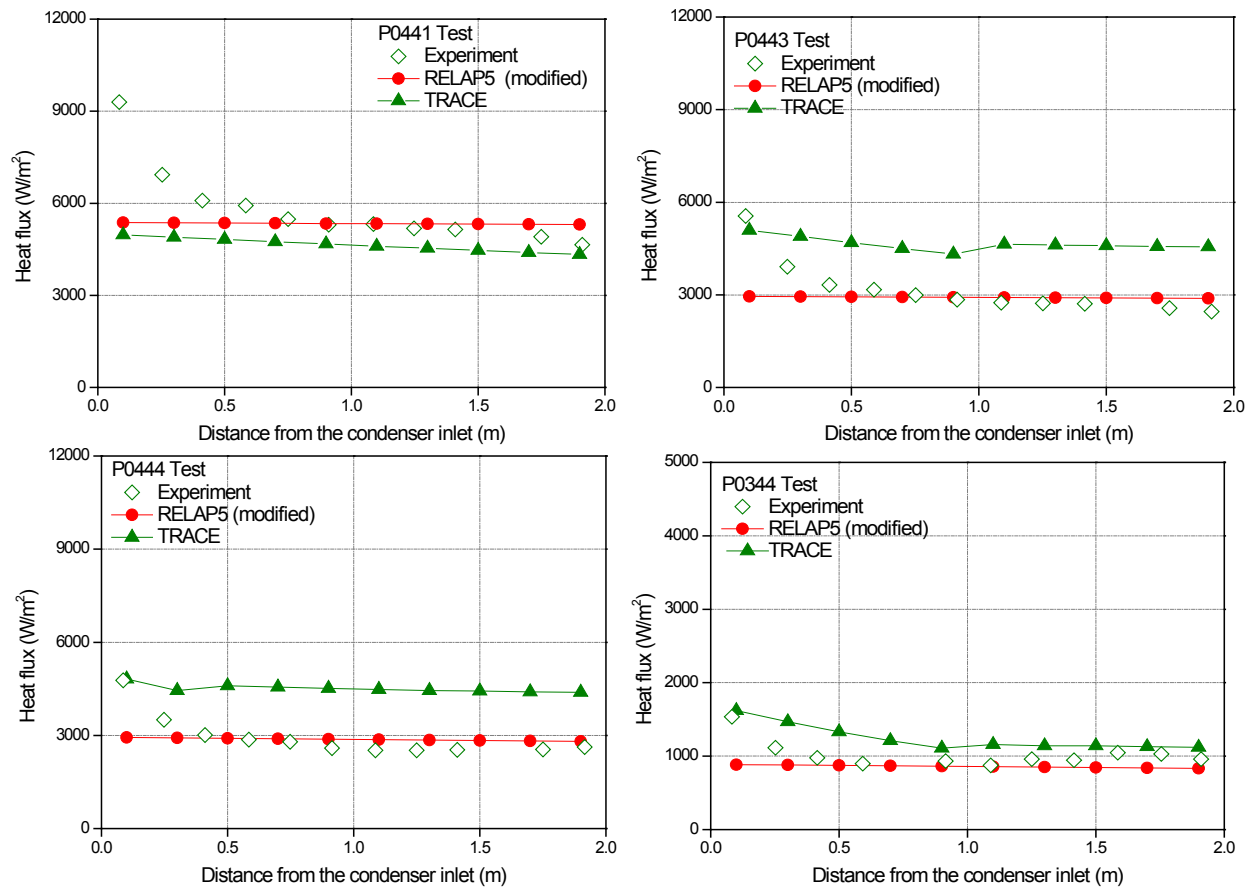


Figure 38 COPAIN Calculation Results (TRACE)

4.2 Analysis of the UW Experiment

As with the RELAP5 analysis, the experimental conditions and variables used were drawn from the analysis part of the TRACE Code Assessment Manual used for the University of Wisconsin experiment (Ref. 10). The experimental conditions and schematic diagram of the experimental apparatus are presented in Table 4 and Figure 6, respectively.

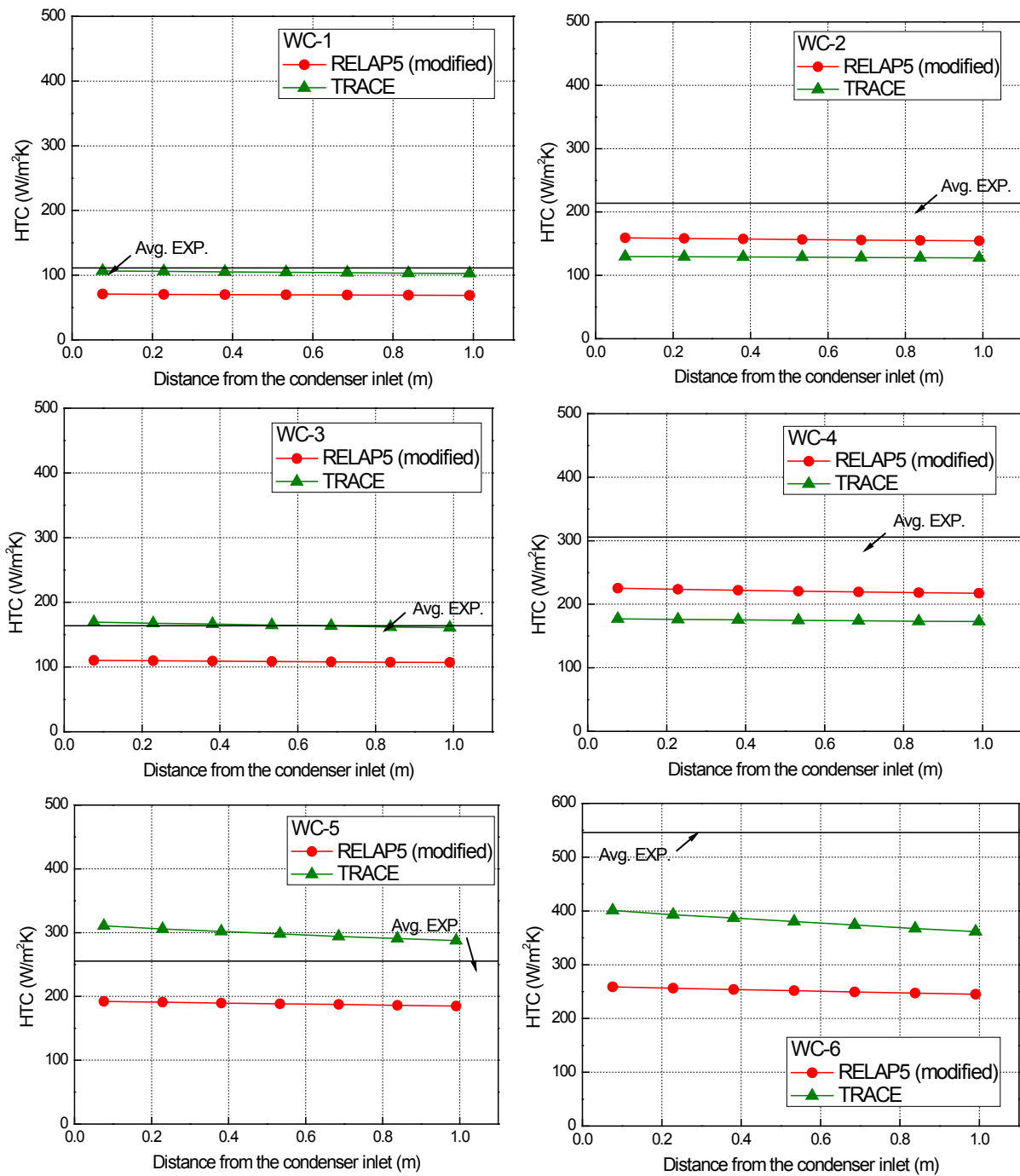


Figure 39 UW Calculation Results (TRACE)

The TRACE and modified RELAP5 calculation results are shown in Figure 39. Because the UW experiment only provided the average heat transfer coefficient, the heat transfer coefficients of TRACE and RELAP5 were compared with the averaged results. In the case of the UW experiment, the condensation heat transfer coefficient of TRACE was predicted to be higher than that of RELAP5 when the gas velocity was slower (WC-1, 3, 5, 6). On the other hand, when the gas velocity was high, the condensation heat transfer coefficient of TRACE was

predicted to be lower (WC-2 and 4). Because the average heat-transfer coefficient was available from the experiment, which includes the inlet effect, the calculation results should be under-predicted in comparison to the experimental results. However, TRACE predicted a higher condensation heat transfer coefficient in some cases. Therefore, it was concluded that TRACE over-predicts the condensation heat transfer in some natural convection conditions.

4.3 Analysis of the CONAN Experiment

Similar to the previous two experiments, the CONAN condensation Benchmark-2 experiments were simulated using TRACE and RELAP5 to verify the prediction performance of the rectangular channel condensation. The experimental conditions and schematic of the experimental apparatus are presented in Table 6 and Figure 10, and the nodalization is the same as that in RELAP5, as shown in Figure 11. The results of the analysis using TRACE and the modified RELAP5 are shown in Figure 40.

Both the modified RELAP5 and TRACE predicted similar quantities of condensation heat flux. Because the CONAN experiments were all under forced convection, the natural-convection heat transfer model was not activated and the over-prediction of the heat flux observed in the previous calculation did not appear.

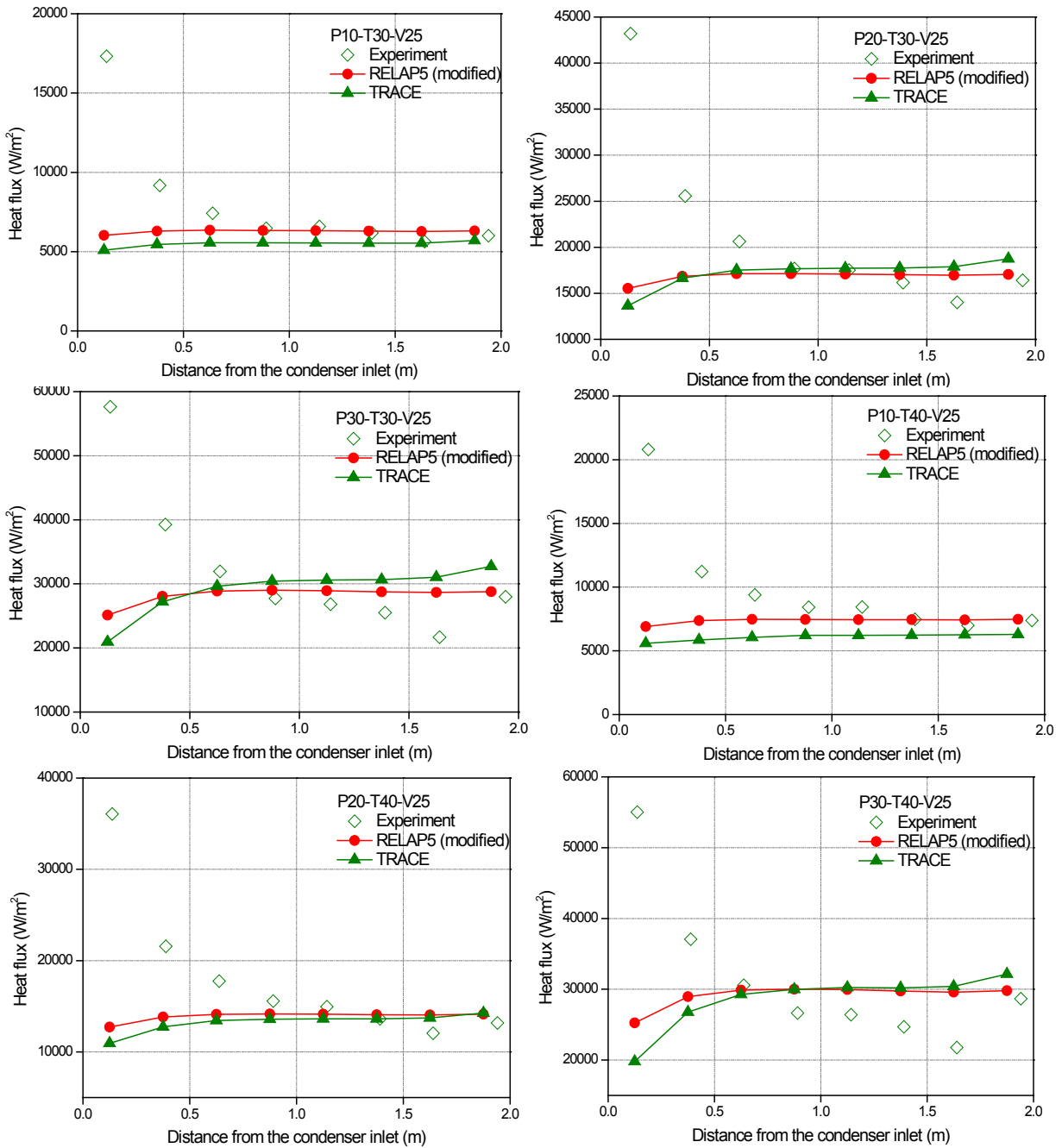


Figure 40 CONAN Calculation Results (TRACE)

The RELAP5 and TRACE calculation results of these three plate wall experiments are presented in Figure 41. In the case of the plate experiments, TRACE overestimates the condensation heat flux in the natural-convection region, as shown in the figures, especially for the COPAIN experiments. This over-prediction could be caused by the mass transfer coefficient model in TRACE under natural-convection conditions, and therefore, a quantitative evaluation of the condensation simulation in the natural-convection regime would be necessary.

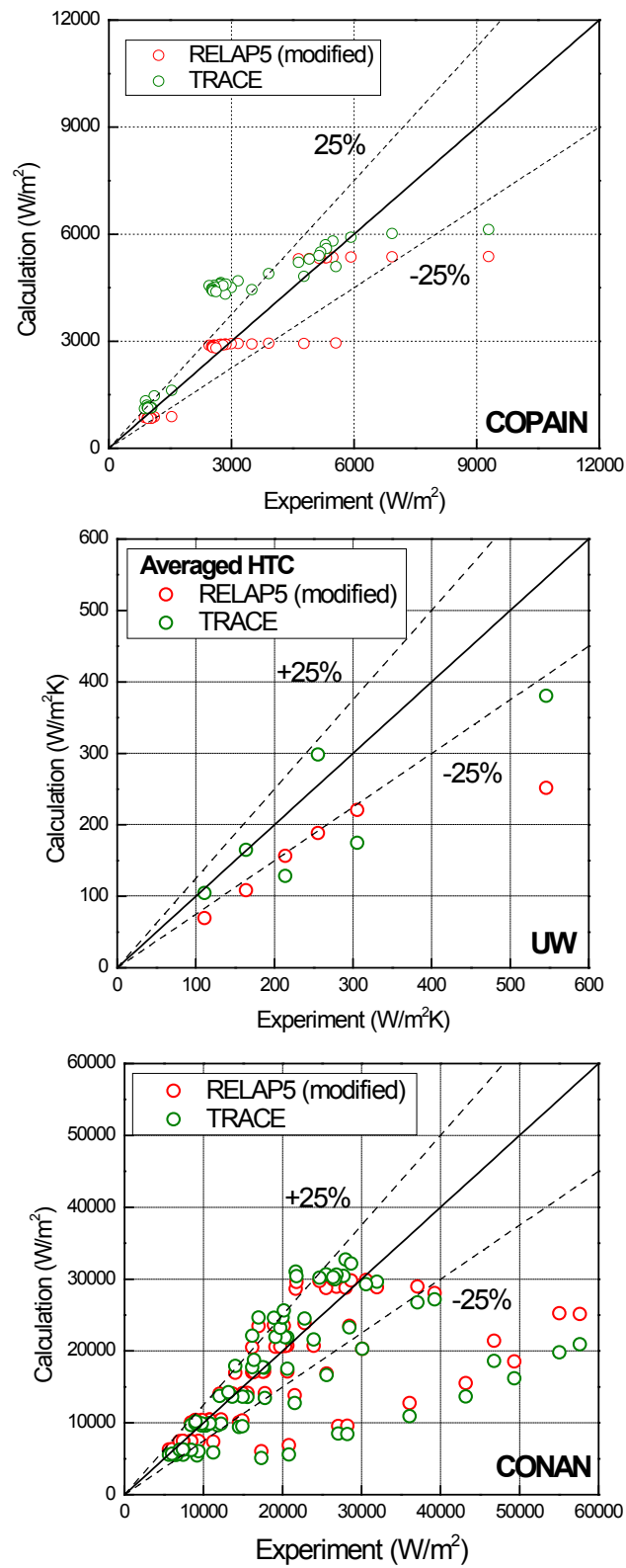


Figure 41 Comparison of RELAP5 and TRACE Results (Plate Experiment)

For the analysis of the tube experiments, four experiments were selected, handled in the same way as for RELAP5, and simulated using the TRACE code.

4.4 Analysis of the MIT Experiment

The experimental conditions of the MIT experiment and schematic of the experimental apparatus are presented in Table 7 and Figure 14, respectively, and the TRACE calculation node is constructed as shown in Figure 15, in the same way as for the RELAP5 nodalization.

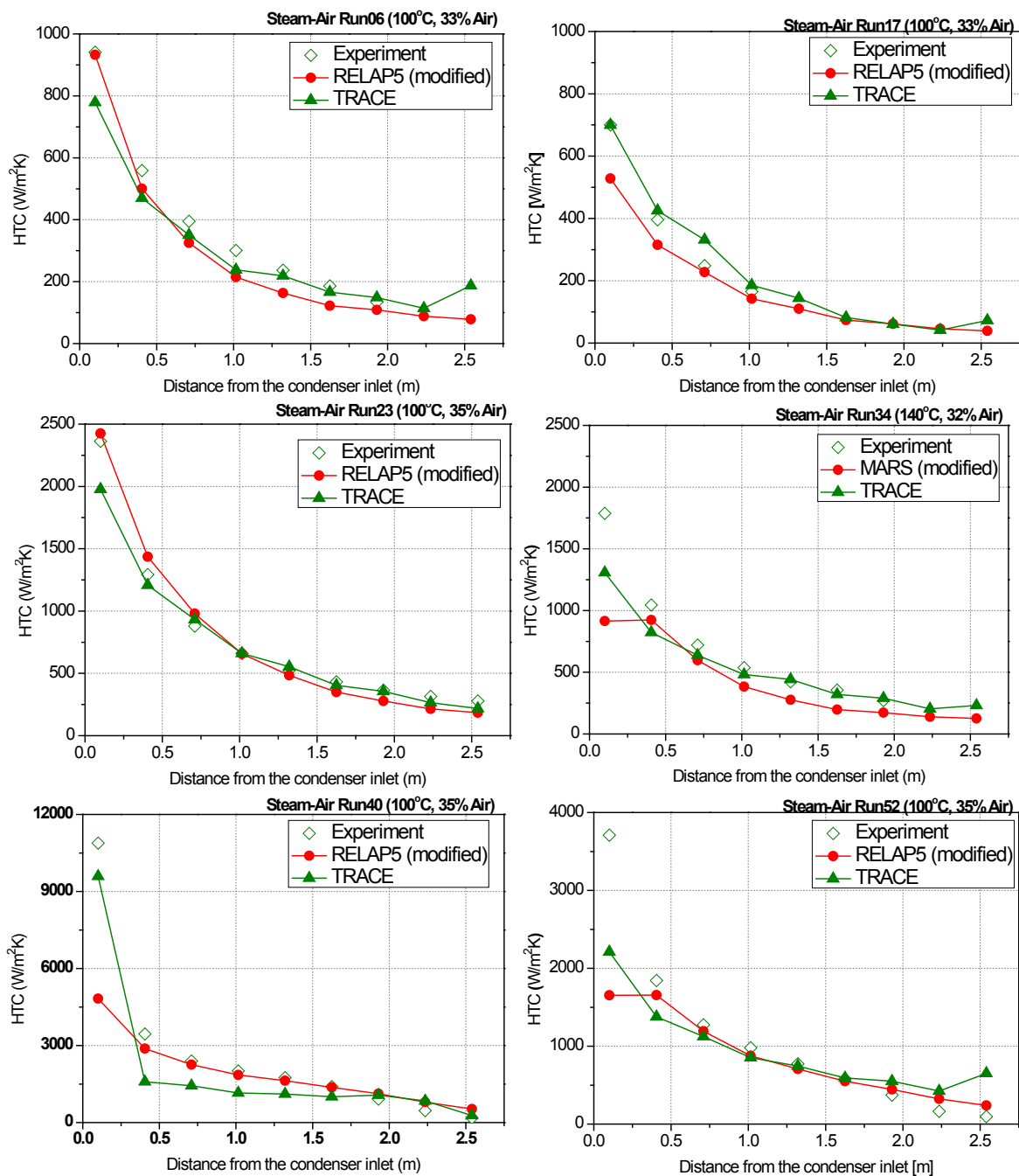


Figure 42 MIT Calculation Results (TRACE)

The analysis results of the MIT experiment using TRACE and the modified RELAP5 are shown in Figure 42. As shown in the figure, the analysis results of TRACE and RELAP5 are comparable to the experimental results. However, as in the lower part of the Run06 experiment, TRACE still over-estimated the condensation heat transfer for natural-convection flows.

4.5 Analysis of the KAIST Experiment

The flow conditions of the KAIST experiment and schematic of the test apparatus are presented in Table 10 and Figure 18, respectively, and the TRACE calculation node was constructed as shown in Figure 19, in the same way as in the RELAP5 nodalization. The results of the KAIST experiment using TRACE and the modified RELAP5 are shown in Figure 43. As shown in the figure, the heat of condensation of the KAIST experimental equipment is reasonably predicted using both codes.

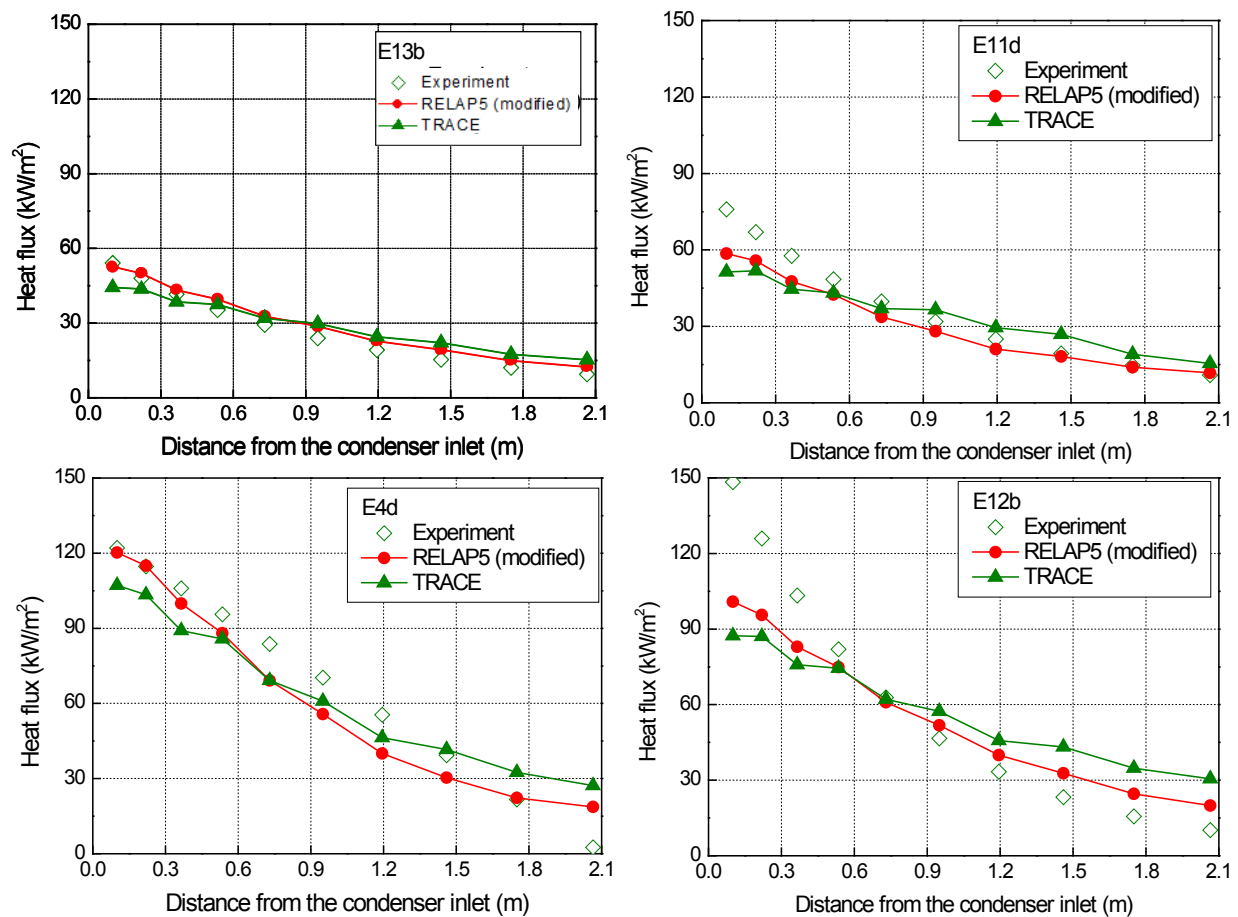


Figure 43 KAIST Calculation Results (TRACE)

4.6 Analysis of the POSTECH Experiment

The POSTECH experimental conditions and schematic of the experimental apparatus are presented in Table 11 and Figure 22, respectively, and the TRACE calculation node was constructed as shown in Figure 23, in the same way as for RELAP5. The results of the POSTECH experiment using TRACE and the modified RELAP5 are shown in Figure 44. According to the TRACE and modified RELAP5 analyses, the condensation heat flux at the

bottom of the condensation wall was relatively accurate. On the other hand, in the case of the experimental analysis with a large steam flow rate, the analysis results near the inlet area showed a larger error in RELAP5 than in TRACE. Although the wall temperature boundary condition was close to the gas mixture temperature, in the case of TRACE, the predicted condensation heat flux was relatively close to the experimental results.

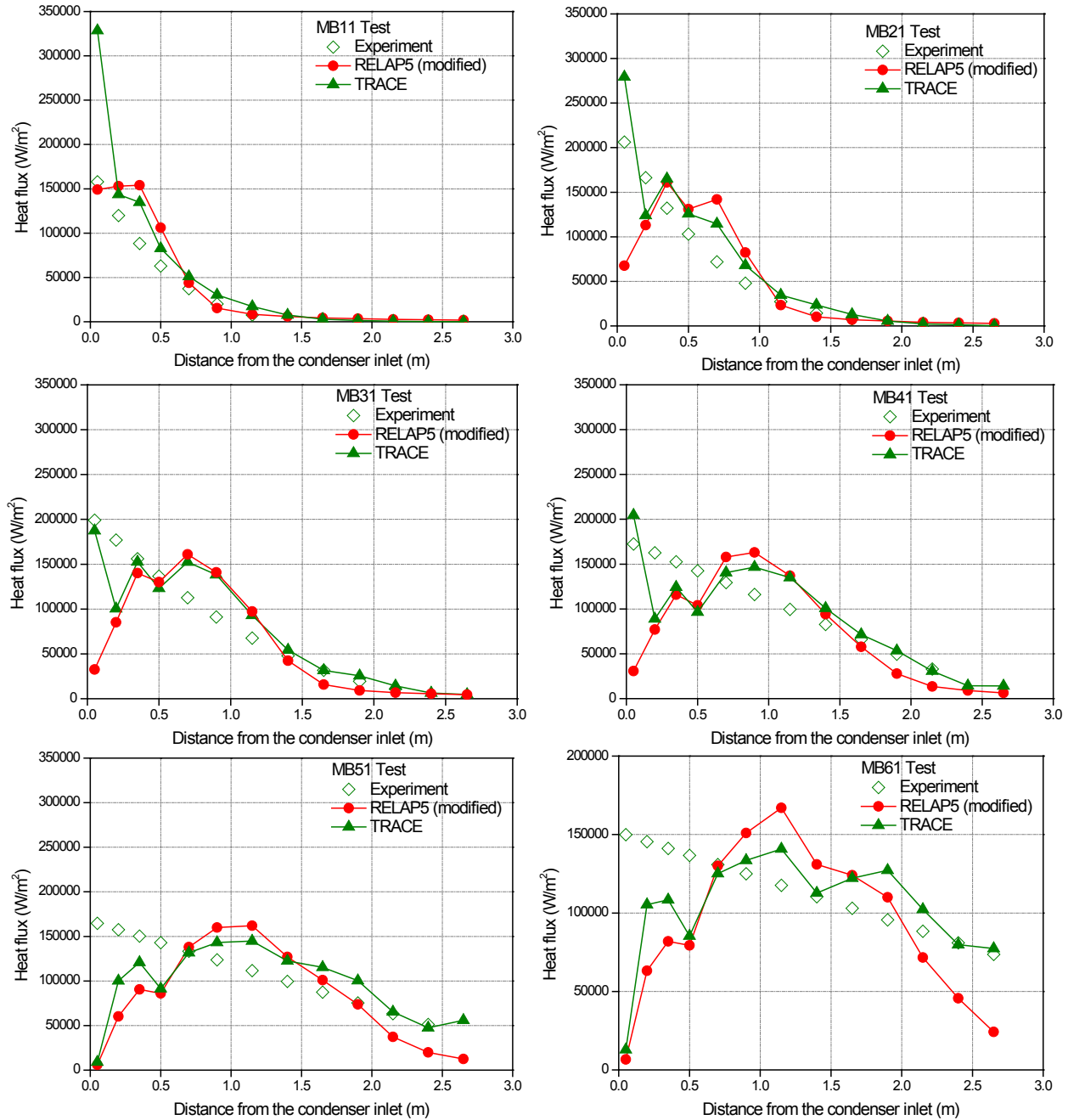


Figure 44 POSTECH Calculation Results (TRACE)

4.7 Analysis of the UCB Experiment

The UCB experimental conditions and schematic of the experimental apparatus are presented in Table 12 and Figure 26, respectively, and the TRACE calculation node was constructed as shown in Figure 27, in the same way as for RELAP5.

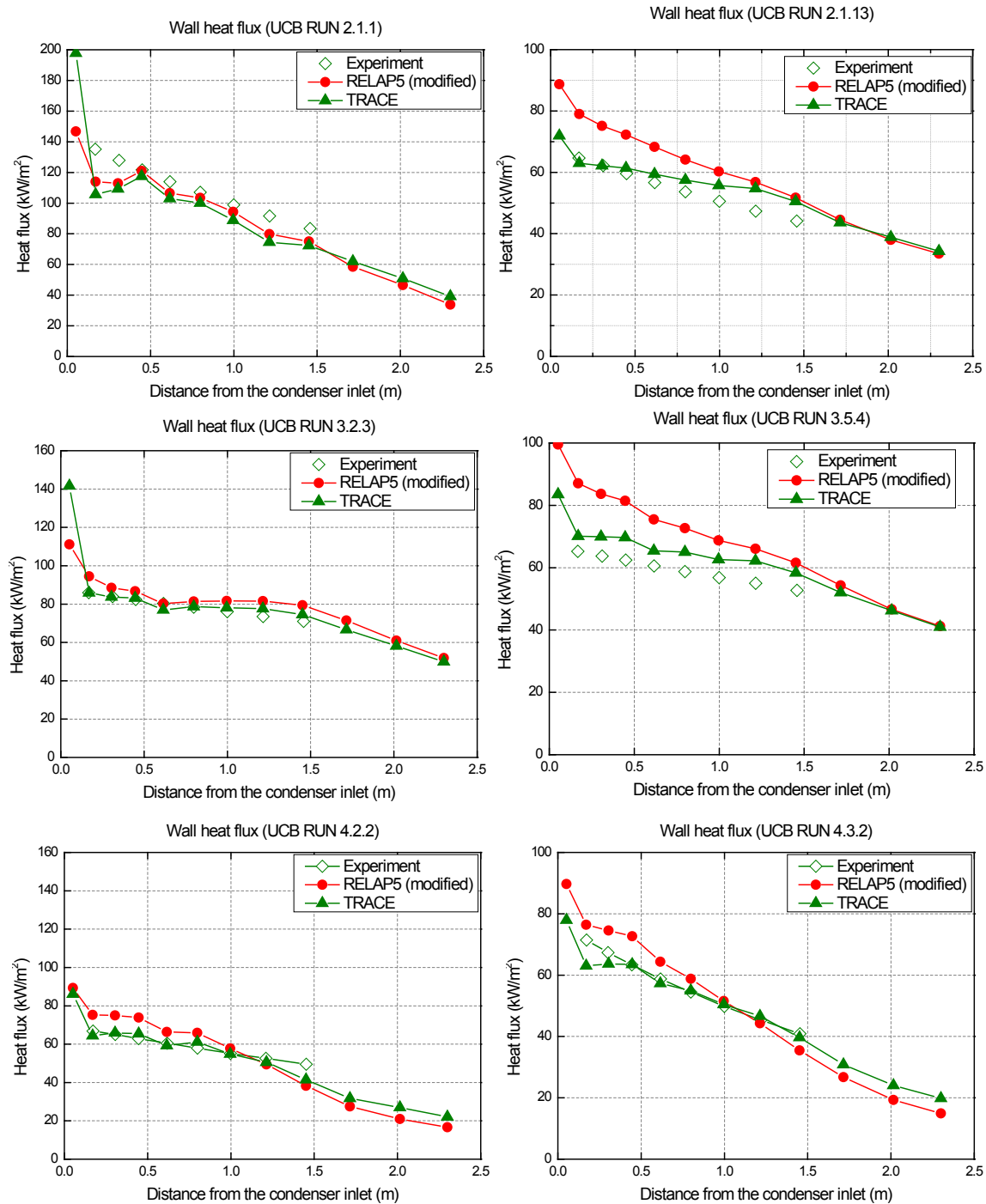


Figure 45 UW Calculation Results (TRACE)

The results of the UCB experiment using TRACE and the modified RELAP5 are shown in Figure 45. According to the analyses, TRACE showed a result in better agreement with the experiment results than that of RELAP5, which over-predicted the heat flux.

The RELAP5 and TRACE results of the previous four experiments are summarized in Figure 46. As shown in the figure, the calculation error is less than that in the plate wall experiment simulations, because the entrance region is shorter in the tube experiments compared to that in the plate wall tests. In addition, the over-prediction of TRACE for the condensation heat flux under natural-convection conditions is smaller than that of the plate type experiment.

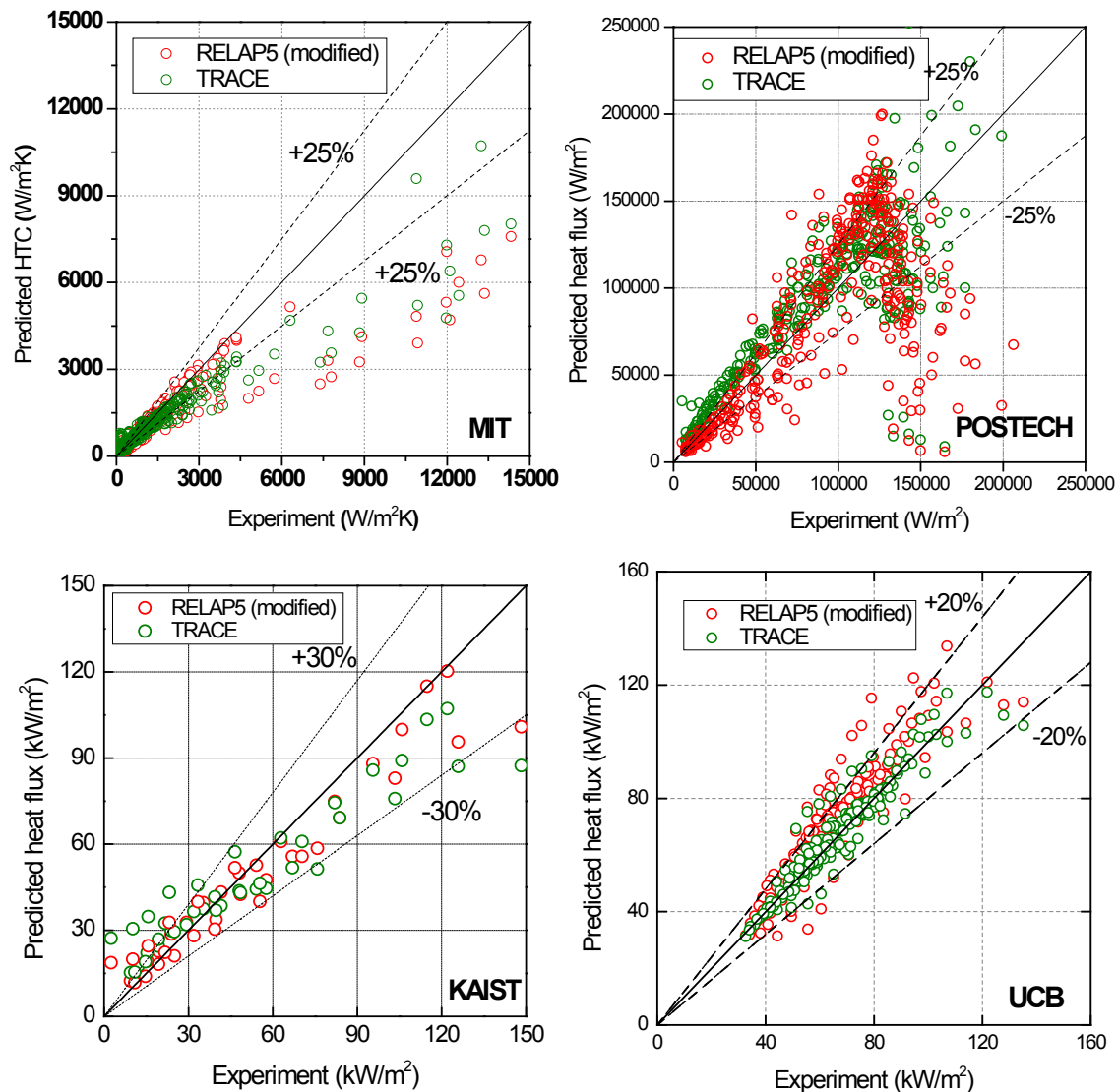


Figure 46 Comparison of RELAP5 and TRACE Results (Tube Experiment)

5 CONCLUSIONS

In this report, models for wall-film condensation in the presence of non-condensable gases used in the nuclear reactor safety analysis codes RELAP5 and TRACE were summarized, and the differences between them were analyzed. An error found during this process was corrected in the source code and the corrected code was assessed with seven experiments to confirm improved prediction ability of the new code. Moreover, it was confirmed that the error in the original RELAP5 affects prediction of the heat flux when the non-condensable gas fraction is high, and does not have a considerable effect when that fraction is low.

In order to quantitatively analyze the difference between the condensation heat transfer models of RELAP5 and TRACE, the same experiments assessed with RELAP5 were analyzed using TRACE. From the plate wall condensation analysis, it was found that the heated diameter needs to be applied to the length scale in the input instead of the hydraulic diameter, in order to prevent a non-physical increase in the heat flux evaluation.

The assessment results showed that the values of heat transfer obtained from those two codes can have considerable discrepancy under natural-convection conditions because different mass transfer coefficient models were implemented for the natural convection. Thus, it was concluded that the condensation heat transfer model under natural-convection conditions needs to be improved to cover a wider range of flow conditions with non-condensable gases.

6 REFERENCES

1. Colburn, A. P., Hougen, O. A., 1934. Design of Cooler Condensers for Mixtures of Vapors with Noncondensing Gases. *Industrial and Engineering Chemistry*, 26, pp. 1178-1182.
2. USNRC, 1998. RELAP5/MOD3 Code Manual Volume I: Code Structure, System Models, and Solution Methods, Information Systems Laboratories, Inc., Rockville, Maryland, Idaho Falls, Idaho.
3. USNRC, 2007. TRACE V5.0 Theory Manual, Field Equations, Solution Methods, and Physical Models, Washington, DC.
4. Grauntt, R. O., et al., 2005. MELCOR Computer Code Manuals – Vol. 2 Reference Manuals. (version 1.8.6), Sandia National Laboratories.
5. Rohsenow, W. M., and Choi, W. M., 1961. *Heat Mass and Momentum Transfer*. New Jersey: Prentice Hall.
6. Churchill, S. W., Chu., H. S., 1975, Correlating Equations for Laminar and Turbulent Free Convection From a Vertical Plate. *International Journal of Heat and Mass Transfer*. 18. pp. 1323-1329.
7. Collier, J. G., Thome, J. R., 1994. *Convective Boiling and Condensation*, 3rd Edition. Clarendon Press, Oxford.
8. Lee, J. H., et al., 2015. Proposal for In-kind Contribution – Assessment of Wall Film Condensation Model in the Presence Of NC Gas using RELAP5 and TRACE. 2015 NRC Spring Meeting Camp.
9. Cheng, X., et al., 2001. Experimental Data Base for Containment Thermal-Hydraulic Analysis. *Nuclear Engineering and Design*, 204, pp.267-284.
10. USNRC, 2007. TRACE V5.0 – Assessment Manual, Appendix B: Separate Effect Tests, Washington, DC.
11. Vyskocil, L., et al., 2014. CFD Simulation of Air-Steam Flow with Condensation. *Nuclear Engineering and Design*, 279, pp.147-157.
12. Siddique, M. S., 1992. The Effect of Noncondensable Gases on Steam Condensation under Forced Convection Condition, Ph.D. dissertation, Massachusetts Institute of Technology.
13. Park, H. S. 1999. Steam Condensation Heat Transfer in the Presence of Noncondensables in a Vertical Tube of Passive Containment Cooling System, Ph.D. dissertation, Korea Advanced Institute of Science and Technology.
14. Lee, K. Y. 2007. The Effects of Noncondensable Gas on Stream Condensation in a Vertical Tube of Passive Residual Heat Removal System, Ph. D. dissertation, Department of Mechanical Engineering, Pohang University of Science and Technology.

15. Kuhn, S. Z. 1995. Investigation of Heat Transfer from Condensing Steam-Gas Mixtures and Turbulent Films Flowing Downward inside a Vertical Tube, Ph. D. dissertation, University of California, Berkeley.
16. Gnielinski, V. 1976. New Equations flow regime Heat and Mass Transfer in Turbulent Pipe and Channel Flow. International Chemical Engineering, 16, pp. 359-368.
17. McAdams, W. H., et al., Heat Transfer at High Rates to Water with Surface Boiling. Industrial Engineering Chemical, 41, pp. 1945-1955.

BIBLIOGRAPHIC DATA SHEET

(See instructions on the reverse)

1. REPORT NUMBER
(Assigned by NRC, Add Vol., Supp., Rev.,
and Addendum Numbers, if any.)

NUREG/IA-0491

2. TITLE AND SUBTITLE

Assessment of the Wall Film Condensation Model with Non-condensable Gas
in RELAP5 and TRACE for Vertical Tube and Plate Geometries

3. DATE REPORT PUBLISHED

MONTH	YEAR
February	2019

4. FIN OR GRANT NUMBER

5. AUTHOR(S)

Jehee Lee*, Chi-Jin Choi*, Hyoung Kyu Cho*, Kyung Won Lee**, Min Ki Cho*

6. TYPE OF REPORT

Technical

7. PERIOD COVERED (Inclusive Dates)

8. PERFORMING ORGANIZATION - NAME AND ADDRESS (If NRC, provide Division, Office or Region, U. S. Nuclear Regulatory Commission, and mailing address; if contractor, provide name and mailing address.)

Department of Nuclear Engineering,
Seoul National University
1 Gwanak-ro, Gwanak-gu, Seoul, 08826, Republic of Korea.

Korea Institute of Nuclear Safety
62 Gwahak-ro-Yuseong-gu
Daejeon, 34142, Korea

9. SPONSORING ORGANIZATION - NAME AND ADDRESS (If NRC, type "Same as above", if contractor, provide NRC Division, Office or Region, U. S. Nuclear Regulatory Commission, and mailing address.)

Division of Systems Analysis
Office of Nuclear Regulatory Research
U.S. Nuclear Regulatory Commission
Washington, D.C. 20555-0001

10. SUPPLEMENTARY NOTES

K. Tien, Project Manager

11. ABSTRACT (200 words or less)

In the interest of providing increased power supply, available passive safety features such as Passive Containment Cooling System (PCCS) and Passive Auxiliary Feedwater System (PAFS) have been adopted for use in advanced nuclear power reactors. The accurate prediction of condensation heat transfer in these systems has been emphasized to assure the safety of nuclear reactors. Especially in the PCCS, condensation occurs in the presence of non-condensable gases that concentrate on the condenser wall. The concentrated gases reduce the steam partial pressure and degrade the heat transfer rate.

In order to predict the condensation rate under this condition, RELAP5 (which is generally used for simulation of best-estimate transients in light water reactor coolant systems) uses the Colburn-Hougen model. Recently, it was found that an error was included in the condensation mass flux model of RELAP5, and the source code of the model was corrected. Next, it was necessary to assess the predictive capability of the corrected model in relation to existing experimental results and in relation to results predicted using another code.

In this study, seven condensation experiments were simulated using RELAP5 and TRACE. These were used to describe condensation on the inner wall of the channel in the presence of non-condensable gases. Then, the predicted heat flux and heat transfer coefficient from both codes were compared with experimental results to evaluate the condensation models

12. KEY WORDS/DESCRIPTORS (List words or phrases that will assist researchers in locating the report.)

Passive Containment Cooling System (PCCS)
Passive Auxiliary Feedwater System (PAFFS)
RELAP5/MOD.3
Methods for Estimation of Leakages and Consequences of Releases (MELCOR)
Korea Radiation Safety Foundation (KORSAFE)

13. AVAILABILITY STATEMENT

unlimited

14. SECURITY CLASSIFICATION

(This Page)

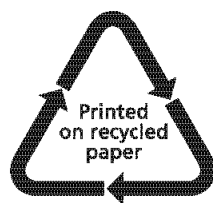
unclassified

(This Report)

unclassified

15. NUMBER OF PAGES

16. PRICE



Federal Recycling Program



UNITED STATES
NUCLEAR REGULATORY COMMISSION
WASHINGTON, DC 20555-0001

OFFICIAL BUSINESS



NUREG/IA-0491

**Assessment of the Wall Film Condensation Model with Non-condensable Gas in RELAP5 and
TRACE for Vertical Tube and Plate Geometries**

February 2019